ELSEVIER

Contents lists available at ScienceDirect

Computers & Industrial Engineering

journal homepage: www.elsevier.com/locate/caie





On multivariate copula modeling of dependent degradation processes

Guanqi Fang a,b,*, Rong Pan c

- ^a School of Statistics and Mathematics, Zhejiang Gongshang University, Hangzhou 310018, China
- b Collaborative Innovation Center of Statistical Data Engineering, Technology & Application, Zhejiang Gongshang University, Hangzhou 310018, China
- ^c School of Computing, Informatics and Decision Systems Engineering, Arizona State University, Tempe, AZ 85281, United States

ARTICLE INFO

Keywords: Degradation process Exchangeable Archimedean copula Elliptical copula Gaussian copula Multivariate model Remaining useful life prediction System reliability Vine copula

ABSTRACT

Multivariate degradation processes have been observed in many engineering systems. Most existing multivariate degradation modeling techniques, such as multivariate general path models or multivariate Wiener process models, assume an underlying Gaussian dependence structure. Unfortunately, in reality, the dependencies among degradation processes are often nonlinear, asymmetric and greatly tail-skewed, and thus limit the usefulness of the conventional modeling techniques in practice. To overcome these limitations, in this paper, we develop a copula-based multivariate modeling framework. Three fundamental copula classes are applied to model the complex dependence structure among correlated degradation processes. Statistical inference and model selection techniques, including two graphical diagnostic tools, a test of independence and a goodness-of-fit test, are employed to identify the best model. The advantages of the proposed modeling framework are demonstrated through simulation studies. And we also discuss the effect of ignoring tail dependence on system failure probability assessment. Finally, the applications of the copula-based multivariate degradation models on both system reliability evaluation and remaining useful life prediction are provided. The proposed methodology is illustrated using a numerical example.

1. Introduction

1.1. Motivation

A general engineering system, either a single-component product with multiple failure modes or a complex structure with multiple components, usually involves with both uncertain and dependent degradation processes. For example, the degradation mechanisms of lightemitting diode (LED) lamps usually contain lumen depreciation, discoloration, lens cracking, and color shift of the LED light output (Yazdan Mehr et al., 2020). These indices are affected by not only chemical reactions happening in the optical components, but both raw manufacturing defects and surrounding service conditions. All of these complexities make the LED perform with uncertainty. And the interactions among some mechanisms - including contribution of both discoloration and lens cracking to color shift - imply the dependence existing in the degradation processes. Similar phenomena exist in many other applications, such as polymeric material (Fang, Pan, & Hong, 2020) and lithium-ion batteries (Peng, Ye, & Chen, 2018). For a complex structure with multiple components, dependencies among the components are often present as well. These dependencies may originate from possible power load and interconnecting pieces shared by the components. See Xu, Wei, Elsayed, Chen, and Kang (2017) and Shen, Zhang, Song, and Song (2019) for some examples. Thus, accounting for the dependencies existing among the performance characteristics (PCs) of a degrading system plays an important role in system reliability assessment.

To evaluate the reliability for such a system, the knowledge about both the system's reliability-wise structure and the probabilistic model of these PCs is needed. The reliability-wise structure describes the system-component configuration, while the probabilistic model defines the statistical behavior of the corresponding multiple PCs. Denote the multiple PCs by a random vector $Y=(Y_1,Y_2,...,Y_d)^{'}$ and let $f(y_1,y_2,...,y_d)$ be its joint probability density function (pdf). In addition, denote the structure function by $g(\cdot)$ and let $\{\mathbb{D}:g(y)=1\}$ represent the domain of a working system. Then, the system reliability can be evaluated by the equation indicated in Fig. 1. It is defined by the multivariate integral of $f(y_1,y_2,...,y_d)$ over the domain \mathbb{D} . In this paper, we consider either a series or parallel structure. Thus, the domain of a working system is simply $\{\mathbb{D}:g(y)=\prod_{i=1}^d 1(y_i<\mathcal{D}_i)=1\}$ and $\{\mathbb{D}:g(y)=\max_{i=1}^d 1(y_i)=1\}$

E-mail addresses: gfang5@asu.edu (G. Fang), rong.pan@asu.edu (R. Pan).

^{*} Corresponding author.

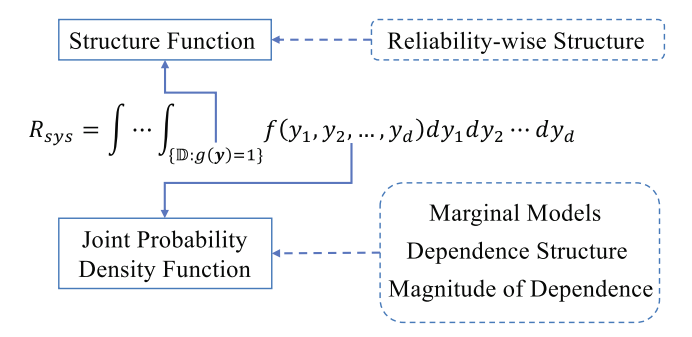


Fig. 1. Characterization of System Reliability.

 $1-\prod_{i=1}^d \mathbf{1}(y_i \geqslant \mathcal{D}_i)=1$ }, respectively. And we assume each PC increases up to \mathcal{D}_i until failure without loss of generality and \mathcal{D}_i is a "soft" failure threshold for process i.

But defining a multivariate joint distribution for multiple PCs imposes a big challenge. As illustrated in Fig. 1, a flexible joint pdf should possess three features - being able to (1) accommodate various marginal distribution models, (2) include a large group of dependency types, and (3) capture possible diverse magnitude of dependency among marginals. Most existing research works either assume PCs to be mutually independent or subject to a specific type of multivariate distribution (Pan & Fang, 2020, chap. 2). Apparently, the independence assumption is not appropriate since marginal degradation processes often have interactions with each other due to their shared operational/environmental conditions or common manufacturing defects, etc (Wang & Li, 2018). On the other hand, assigning a symmetric multivariate distribution, usually a multivariate normal distribution or multivariate Student's t distribution, may not fit the actual multivariate degradation process well. This is because the adopted Gaussian dependence structure cannot capture the nonlinear dependency or the tail dependency that may exist among PCs (Wang & Li, 2017). As a result, the system reliability assessment could be biased due to model misspecification. But it is also difficult to construct a multivariate distribution beyond the Gaussian-based distribution model, say the multivariate gamma distribution, while maintaining nice statistical properties. Thus, a flexible multivariate distribution construction method is much desired to help quantify reliability for systems with dependent degradation processes. The main goal of this paper is therefore to expand stochastic degradation process models to the multivariate domain and to improve the applicability of the developed methods in practice.

1.2. Literature review

In literature, there are a lot of research works discussing the distribution models of univariate degradation processes. In general, two types of modeling framework are available – the general path model and the stochastic process model (Ye & Xie, 2015). The general path model is a regression-based model that can easily take the unit-to-unit variability into account. For instance, Fang, Rigdon, and Pan (2018) proposed a nonlinear mixed-effects model to analyze the accelerated degradation testing (ADT) data of optical media. Bae and Kvam (2004) provided a general form of random-coefficients model to incorporate both within-individual and between-individual variation. Alternatively, the stochastic process model extends the distribution types by considering the Wiener process (Ye, Wang, Tsui, & Pecht, 2013; Zhai & Ye, 2017; D. He, Wang, & Cao, 2018; L. He, Yue, & He, 2018), the gamma process (Castro & Landesa, 2019; Lawless & Crowder, 2004), and the inverse Gaussian (IG) process (Peng, 2015; Ye & Chen, 2014).

When dealing with a multivariate degradation process, there are two major approaches – a direct extension from existing univariate models to multivariate versions and a copula-based multivariate modeling approach. For example, Lu, Wang, Hong, and Ye (2020) proposed a

multivariate general path model to analyze a trivariate polymeric degradation process. Wang, Balakrishnan, and Guo (2015) utilized a multivariate Wiener process to analyze three-dimensional degradation data. Nevertheless, both the multivariate general path model and the multivariate Wiener process model still belong to the Gaussian-based distribution, which contains the potential drawbacks as mentioned before. To resolve the issues, in recent years, the copula-based modeling framework has gained lots of interests due to its flexibility. But most existing works about copula-based models mainly focus on bivariate analysis, e.g. (Fang et al., 2020; Pan & Balakrishnan, 2011; Peng, Li, Yang, Zhu, & Huang, 2016; Wang, Balakrishnan, Guo, & Jiang, 2015; Wu, 2014). Until recently, some practical research works of multivariate copula-based degradation models are available. For instance, Xu et al. (2017) utilized a vine copula to analyze high-dimensional data produced by a smart electricity meter. Sun, Fu, Liao, and Xu (2020) utilized the Wiener process model and a vine copula to analyze the ADT data of a tuner. However, to our best knowledge, there is a lack of complete systematic studies on how to apply multivariate copula models on analyzing dependent degradation processes, nor a comparison among these models. This paper is to fill these gaps.

1.3. Overview

Three primary contributions are made in this paper. First, we provide a systematic approach to investigating the multivariate copula modeling of dependent degradation processes. It includes comparing three fundamental copula classes in the process of multivariate dependency modeling, along with a tailored workflow of statistical inference and model selection, which includes two graphical diagnostic methods, a test of independence, and a goodness-of-fit (GOF) test. Second, a comparison between the tail-dependent Gumbel copula and the widely-used Gaussian copula is made. It contains a study of the effect of ignoring tail dependence on system failure probability assessment. Finally, the applications of the copula-based multivariate degradation models on both system reliability evaluation and remaining useful life prediction are provided. The proposed methodology is illustrated using a numerical example.

The rest of the paper is organized as follows. Section 2 illustrates the copula theory and the three fundamental classes of copula models. Section 3 discusses the modeling framework of dependent degradation processes. Specifically, Section 3.1 introduces the marginal degradation models and Section 3.2 provides a framework of incorporating the marginal models into the aforementioned multivariate copula models. Section 4 illustrates the applications of both reliability evaluation and online RUL prediction. Then, Section 5 provides a method of statistical inference and a workflow of model selection. In Section 6, simulation studies are given to demonstrate model characteristics and study the effect of model misspecification. Finally, a numerical example is provided in Section 7. Section 8 concludes this paper.

2. Multivariate copula models

In this section, we introduce the copula theory as well as the three fundamental classes of copula model.

2.1. Copula theory

A copula, $C(\cdot)$, is a multivariate cumulative distribution function (cdf) with standard univariate uniform margins. Mathematically, it is defined as (Nelsen, 2007)

$$C(\mathbf{u}) = C(u_1, u_2, ..., u_d) = P(U_1 \leqslant u_1, U_2 \leqslant u_2, ..., U_d \leqslant u_d),$$

where $u = (u_1, u_2, ..., u_d)^{'} \in R^d$ and $U = (U_1, U_2, ..., U_d)^{'}$ is a d-dimensional random vector with $U_i \sim \textit{Unif}(0, 1), \forall i = 1, 2, ..., d$. As a multivariate distribution function, its properties including the joint, marginal,

and conditional functions along with survival copula are available as summarized by the part of Copula Scale: u in Table 3 that is presented in Appendix.

Since a copula function is with respect to uniformly distributed margins, we may treat an individual margin as the cdf of any continuous marginal distribution so as to represent a general continuous multivariate distribution. This well-known Sklar's theorem is stated as below:

Sklar's Theorem (Nelsen, 2007): Let $X = (X_1, X_2, ..., X_d)^{'}$ be a random vector with marginal cdfs, $F_1(x_1), F_2(x_2), ..., F_d(x_d)$, and let $F(x_1, x_2, ..., x_d)$ be their joint cdf. Define $u_i = F_i(x_i) = P(X_i \leqslant x_i), \forall i = 1, 2, ..., d$. Then, there exists a copula function $C(\cdot)$ such that

$$C(u_1, u_2, ..., u_d) = C(F_1(x_1), F_2(x_2), ..., F_d(x_d))$$

$$= P(X_1 \leq x_1, X_2 \leq x_2, ..., X_d \leq x_d)$$

$$= F(x_1, x_2, ..., x_d).$$

Note that in some literature, $F(x_1, x_2, ..., x_d)$ is denoted by $H(x_1, x_2, ..., x_d)$. With the cdf of a joint distribution, it is easy to derive the joint pdf as

$$f(x_{1}, x_{2}, ..., x_{d})$$

$$= \frac{\partial^{d} F(x_{1}, x_{2}, ..., x_{d})}{\partial x_{1} \partial x_{2} \cdots \partial x_{d}}$$

$$= \frac{\partial^{d} C(F_{1}(x_{1}), F_{2}(x_{2}), ..., F_{d}(x_{d}))}{\partial F_{1}(x_{1}) \partial F_{2}(x_{2}) \cdots \partial F_{d}(x_{d})} \frac{\partial F_{1}(x_{1})}{\partial x_{1}} \frac{\partial F_{2}(x_{2})}{\partial x_{2}} \cdots \frac{\partial F_{d}(x_{d})}{\partial x_{d}}$$

$$= c(F_{1}(x_{1}), F_{2}(x_{2}), ..., F_{d}(x_{d})) \prod_{i=1}^{d} f_{i}(x_{i}),$$

$$(1)$$

where $f_i(x_i)$ is the marginal pdf of X_i and $c(F_1(x_1),F_2(x_2),...,F_d(x_d))$ is the copula density, which can be obtained by taking partial derivatives of the copula. Notice that if all marginals are mutually independent, $c(F_1(x_1),F_2(x_2),...,F_d(x_d))=1$ since taking partial derivatives of independence copula (i.e. $C(u_1,u_2,...,u_d)=\prod_{i=1}^d u_i$) results in 1. In such case, $f(x_1,x_2,...,x_d)=\prod_{i=1}^d f_i(x_i)$, which matches the conclusion by the independence assumption of random variables. In addition, the conditional pdf and the conditional cdf are given by

$$f\left(x|\mathbf{x}^{*}\right) = c_{x,x_{j}|\mathbf{x}_{-j}^{*}}\left(F\left(x|\mathbf{x}_{-j}^{*}\right), F\left(x_{j}|\mathbf{x}_{-j}^{*}\right)\right) f\left(x|\mathbf{x}_{-j}^{*}\right), \tag{2}$$

$$F(x|\mathbf{x}^*) = \frac{\partial C_{x,y_j|\mathbf{x}_{-j}^*} \left(F(x|\mathbf{x}_{-j}^*), F(x_j|\mathbf{x}_{-j}^*) \right)}{\partial F(x_j|\mathbf{x}_{-j}^*)},$$
(3)

where x^* is a (d-1)-dimensional vector of random variables without x. x_j is one arbitrary element of x^* and x_{-j}^* denotes the vector excluding this element. Note that in a bivariate case, the joint pdf, conditional pdf and conditional cdf are sequentially given by

$$f(x_1, x_2) = c(F_1(x_1), F_2(x_2))f_1(x_1)f_2(x_2),$$
(4)

$$f_{1|2}(x_1|x_2) = \frac{f(x_1, x_2)}{f_2(x_2)} = c(F_1(x_1), F_2(x_2))f_1(x_1),$$
(5)

$$F_{1|2}(x_1|x_2) = C(F_1(x_1)|F_2(x_2)) = \frac{\partial C(F_1(x_1), F_2(x_2))}{\partial F_2(x_2)}.$$
 (6)

These properties for the original variables (on the scale of x) are also presented in Table 3.

Thus far, it is noted that the copula theory provides a way to construct a joint distribution function. It is done by defining all marginal distributions first and then combining these margins by a copula function. As implied by Eq. (1), the joint density consists of two separate parts – marginal densities and a copula density that characterizes the dependence among the margins. The feature of separation is different from the traditional multivariate distribution specification. Next, we introduce the three fundamental classes of copula functions, which are

elliptical copulas (ECs), exchangeable Archimedean copulas (EACs), and vine copulas (VCs).

2.2. Elliptical copulas

ECs are the copulas of elliptically contoured (or elliptical) distributions. The most commonly-used ones are the Gaussian copula and Student's t copula. Let Φ^{-1} denote the inverse of the cdf of a standard univariate normal distribution Φ and Φ_{Σ} is the d-dimensional standard normal distribution with correlation matrix Σ . Then, the Gaussian copula is given by

$$C(\boldsymbol{u};\boldsymbol{\Sigma}) = \Phi_{\boldsymbol{\Sigma}}(\Phi^{-1}(u_1),\Phi^{-1}(u_2),...,\Phi^{-1}(u_d)).$$

And with I being an identity matrix, its density is

$$c(\boldsymbol{u}; \boldsymbol{\Sigma}) = \frac{1}{|\boldsymbol{\Sigma}|^{\frac{1}{2}}} \exp \left\{ -\frac{1}{2} \begin{bmatrix} \boldsymbol{\Phi}^{-1}(\boldsymbol{u}_1) \\ \vdots \\ \boldsymbol{\Phi}^{-1}(\boldsymbol{u}_d) \end{bmatrix}' (\boldsymbol{\Sigma}^{-1} - \boldsymbol{I}) \begin{bmatrix} \boldsymbol{\Phi}^{-1}(\boldsymbol{u}_1) \\ \vdots \\ \boldsymbol{\Phi}^{-1}(\boldsymbol{u}_d) \end{bmatrix} \right\}.$$

The Student's t copula is constructed similarly. Let T_{ν}^{-1} denote the inverse of the cdf of the standard univariate Student's t distribution T_{ν} with degrees of freedom $\nu>2$ and $T_{\Sigma,\nu}$ is the d-dimensional standardized Student's t distribution with correlation matrix t. Then, the Student's t copula is given by

$$C(\mathbf{u}; \mathbf{\Sigma}, \nu) = T_{\mathbf{\Sigma}, \nu}(T_{\nu}^{-1}(u_1), T_{\nu}^{-1}(u_2), ..., T_{\nu}^{-1}(u_d)),$$

and its density is

$$c(\pmb{u};\pmb{\Sigma},\nu) = \frac{\Gamma[(\nu+d)/2]}{\Gamma(\nu/2)\nu^{d/2}\pi^{d/2}|\pmb{\Sigma}|^{\frac{1}{2}}} \left\{ 1 + \frac{1}{\nu} \begin{bmatrix} T_{\nu}^{-1}(u_1) \\ \vdots \\ T_{\nu}^{-1}(u_d) \end{bmatrix} \mathbf{\Sigma}^{-1} \begin{bmatrix} T_{\nu}^{-1}(u_1) \\ \vdots \\ T_{\nu}^{-1}(u_d) \end{bmatrix} \right\}^{-(\nu+d)/2}.$$

2.3. Exchangeable Archimedean copulas

Archimedean copulas are constructed via a completely different route without referring to a known distribution function or random variable (Yan, 2006). They are produced by a continuous strictly decreasing function $\varphi(\cdot)$ mapping from [0,1] to $[0,\infty]$ with $\varphi(0)=\infty$ and $\varphi(1)=0$. The function is called generator function and denote its inverse by $\varphi^{-1}(\cdot)$. A d-dimensional Archimedean copula is

$$C(\mathbf{u};\delta) = \varphi^{-1}(\varphi(u_1) + \varphi(u_2) + \cdots + \varphi(u_d);\delta),$$

where δ is the association parameter controlling the degree of dependence. For instance, $\varphi(t)=(-\ln(t))^{\delta}$ and $\varphi(t)=(t^{-\delta}-1)/\delta$ are generator functions for the Gumbel copula and Clayton copula, respectively.

Table 4 in Appendix lists the commonly-used copula functions, including the two ECs described before and three EACs, i.e. the Frank copula, Clayton copula, and Gumbel copula. These copulas hold various types of tail dependence: the Gumbel copula has upper-tail dependence (λ_U), the Clayton copula has lower-tail dependence (λ_L), and the Frank copula is symmetric with no tail dependence.

2.4. Vine copulas

Finally, VCs utilize the expression of full conditional distribution for a general multivariate distribution. For instance, for a 3-dimensional case, the joint pdf can be expressed by

$$f(x_1, x_2, x_3) = f_1(x_1) f_{2|1}(x_2|x_1) f_{3|1,2}(x_3|x_1, x_2).$$

Since the conditional pdf can be represented by the product of a copula density and a marginal using Eqs. (1) and (2), the joint pdf above further becomes

$$f(x_{1}, x_{2}, x_{3}) = f_{1}(x_{1}) \cdot f_{2}(x_{2}) \cdot f_{3}(x_{3}) \cdot c_{1,2}(F_{1}(x_{1}), F_{2}(x_{2})) \cdot c_{2,3}(F_{2}(x_{2}), F_{3}(x_{3})) \cdot c_{1,3|2}(F_{1|2}(x_{1}|x_{2}), F_{3|2}(x_{3}|x_{2})).$$

$$(7)$$

This demonstrates that this joint pdf can be constructed by the product of its marginals, two unconditional bivariate copula densities and a conditional bivariate copula density. Aas, Czado, Frigessi, and Bakken (2009) refer to this operation as Pair-Copula Construction (PCC). Formally, PCC in *d*-dimensional is given by

$$\begin{split} &f(\mathbf{x}_1, \mathbf{x}_2, \dots, \mathbf{x}_d) \\ &= f_1(\mathbf{x}_1) f_{2|1}(\mathbf{x}_2|\mathbf{x}_1) \cdots f_{d|1,\dots,d-1}(\mathbf{x}_d|\mathbf{x}_1, \dots, \mathbf{x}_{d-1}) \\ &= \underbrace{\prod_{j=1}^{d-1} \prod_{i=1}^{d-j} c_{i,(i+j)|(i+1),\dots,(i+j-1)}}_{\text{pair-copula densities}} \underbrace{\prod_{k=1}^{d} f_k(\mathbf{x}_k)}_{\text{marginal densities}}, \end{split}$$

where $c_{i,j|i_1,\dots,i_k} = c_{i,j|i_1,\dots,i_k} \left(F_{i|i_1,i_2,\dots,i_k}, F_{j|i_1,i_2,\dots,i_k} \right)$ and $F_{i|i_1,i_2,\dots,i_k} = F_{i|i_1,i_2,\dots,i_k} \left(x_i \middle| x_{i_1}, x_{i_2},\dots, x_{i_k} \right)$ for i,j,i_1,i_2,\dots,i_k with i < j and $i_1 < i_2 < \dots < i_k$. Obviously, the way of decomposition is not unique. To organize the representation, Bedford and Cooke (2001) introduce a

dimensional vine is a sequence of d-1 trees that has the following properties: (1) Tree j has d+1-j nodes and d-j edges; (2) Edges in tree j becomes nodes in tree j+1; and (3) Proximity condition: Two nodes in tree j+1 are joined by an edge if the corresponding edges in tree j share a node.

According to this definition, the joint density represented by a vine consists of pair-copula (bivariate copula) densities over the $\frac{d(d-1)}{2}$ edges of the entire graph and the marginal densities of the d nodes in the first-level tree. Among many different PCC methods, there are two special types of organized vines – the canonical vine (C-vine) and drawable vine (D-vine). For a C-vine, each tree has a unique node that is connected to all other nodes. For a D-vine, each tree is a path. Fig. 2 demonstrates both the C-vine and the D-vine representations for four dependent variables, respectively. If constructed by a C-vine or D-vine, the joint pdfs and cdfs are given as below. In these equations, the conditional cdfs can be calculated using Eq. (3) and the partial derivatives of some commonly-used bivariate copulas are provided in Table 5 that is presented in Appendix. Note that the first partial derivative of a copula function is also called h-function in some literature.

$$\begin{aligned} \text{C--vine:} \begin{cases} f(x_1, x_2, x_3, x_4) &= & f_1(x_1) \cdot f_2(x_2) \cdot f_3(x_3) \cdot f_4(x_4) \cdot \\ & c_{1,2} \cdot c_{1,3} \cdot c_{1,4} \cdot \\ & c_{2,3|1} \cdot c_{2,4|1} \cdot c_{3,4|1,2} \\ & F(x_1, x_2, x_3, x_4) &= & F_1(x_1) F_{2|1}(x_2|x_1) F_{4|1,2}(x_4|x_1, x_2) F_{3|1,2,4}(x_3|x_1, x_2, x_4) \\ &= & F_1(x_1) \frac{\partial C_{1,2} \left(F_1 \left(x_1 \right), F_2 \left(x_2 \right) \right)}{\partial F_1(x_1)} \frac{\partial C_{2,4|1} \left(F_{2|1} \left(x_2 | x_1 \right), F_{4|1} \left(x_4 | x_1 \right) \right)}{\partial F_{2|1}(x_2|x_1)} \cdot \\ & \frac{\partial C_{3,4|1,2} \left(F_{3|1,2} \left(x_3 | x_1, x_2 \right), F_{4|1,2} \left(x_4 | x_1, x_2 \right) \right)}{\partial F_{4|1,2} \left(x_4 | x_1, x_2 \right)} \cdot \\ \\ D - \text{vine:} \begin{cases} f(x_1, x_2, x_3, x_4) &= & f_1(x_1) \cdot f_2(x_2) \cdot f_3(x_3) \cdot f_4(x_4) \cdot \\ & c_{1,2} \cdot c_{2,3} \cdot c_{3,4} \cdot \\ & c_{1,3|2} \cdot c_{2,4|3} \cdot c_{1,4|2,3} \\ & c_{1,3|2} \cdot c_{2,4|3} \cdot c_{1,4|2,3} \end{cases} \\ &= & F_1(x_1) \frac{\partial C_{1,2} \left(F_1 \left(x_1 \right), F_2 \left(x_2 \right) \right)}{\partial F_1(x_1)} \frac{\partial C_{2,3|1} \left(F_{2|1} \left(x_2 | x_1 \right), F_{3|1} \left(x_3 | x_1 \right) \right)}{\partial F_{2|1} \left(x_2 | x_1 \right)} \cdot \\ &= & \frac{\partial C_{1,4|2,3} \left(F_{1|2,3} \left(x_1 | x_2, x_3 \right), F_{4|2,3} \left(x_4 | x_2, x_3 \right) \right)}{\partial F_{1|2,3} \left(x_1 | x_2, x_3 \right)} \cdot \\ &= & \frac{\partial C_{1,4|2,3} \left(F_{1|2,3} \left(x_1 | x_2, x_3 \right), F_{4|2,3} \left(x_4 | x_2, x_3 \right) \right)}{\partial F_{1|2,3} \left(x_1 | x_2, x_3 \right)} \cdot \\ &= & \frac{\partial C_{1,4|2,3} \left(F_{1|2,3} \left(x_1 | x_2, x_3 \right), F_{4|2,3} \left(x_4 | x_2, x_3 \right) \right)}{\partial F_{1|2,3} \left(x_1 | x_2, x_3 \right)} \cdot \\ &= & \frac{\partial C_{1,4|2,3} \left(F_{1|2,3} \left(x_1 | x_2, x_3 \right), F_{4|2,3} \left(x_4 | x_2, x_3 \right) \right)}{\partial F_{1|2,3} \left(x_1 | x_2, x_3 \right)} \cdot \\ &= & \frac{\partial C_{1,4|2,3} \left(F_{1|2,3} \left(x_1 | x_2, x_3 \right), F_{4|2,3} \left(x_4 | x_2, x_3 \right) \right)}{\partial F_{1|2,3} \left(x_1 | x_2, x_3 \right)} \cdot \\ &= & \frac{\partial C_{1,4|2,3} \left(F_{1|2,3} \left(x_1 | x_2, x_3 \right), F_{4|2,3} \left(x_4 | x_2, x_3 \right) \right)}{\partial F_{1|2,3} \left(x_1 | x_2, x_3 \right)} \cdot \\ &= & \frac{\partial C_{1,4|2,3} \left(F_{1|2,3} \left(x_1 | x_2, x_3 \right), F_{4|2,3} \left(x_4 | x_2, x_3 \right) \right)}{\partial F_{1|2,3} \left(x_1 | x_2, x_3 \right)} \cdot \\ &= & \frac{\partial C_{1,4|2,3} \left(F_{1,2,3} \left(x_1 | x_2, x_3 \right), F_{2,2,3} \left(x_1 | x_2, x_3 \right) \right)}{\partial F_{1,2,3} \left(x_1 | x_2, x_3 \right)} \cdot \\ \\ &= & \frac{\partial C_{1,4|2,3} \left(F_{1,2,3} \left(x_1 | x_2, x_3 \right), F_{2$$

graphical structure called regular vine to visualize the multivariate distribution construction process.

Definition of Regular Vine (Bedford & Cooke, 2002): A d-

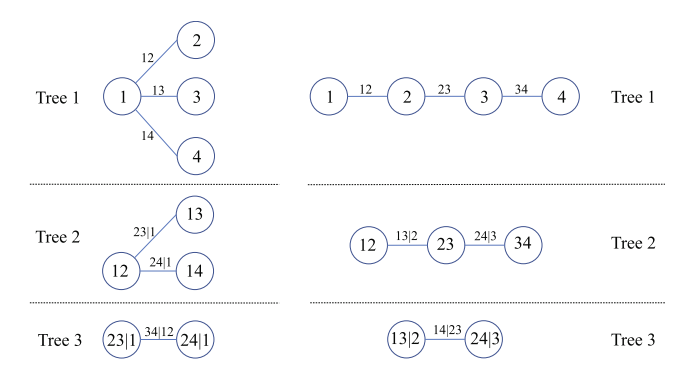


Fig. 2. C-vine (left) and D-vine (right).

3. Distribution modeling of dependent degradation processes

In this section, the marginal degradation models and copula-based joint model are presented.

3.1. Marginal degradation models

Consider a system that may degrade over time due to d degradation processes and each process i, i=1,2,...,d, demonstrates stochastic change over time. In a period of time t_m , the inspection of a degradation variable is taken at ordered times $\{t_{i1},t_{i2},...,t_{ij},...,t_{im}\}$, where m is the total number of inspections on each variable and the subscript j is used as an index associated with the inspection time t_{ij} . Let y_{ij} or $y_i(t_j), i=1,2,...,d$ and j=1,2,...,m, denote the observed degradation value of process i at time point j. Thus, the measurements $\{y_{i1},y_{i2},...,y_{im}\}$ are the resulted observations from the i-th marginal degradation process (MDP) over time.

To model a MDP, three stochastic process models - the Wiener

process, gamma process and IG process – are favored due to their stochastic nature of capturing the natural randomness of system degradation over time (Ye & Xie, 2015). In this paper, we consider these three stochastic processes as candidate models for a MDP. Under these models, the degradation process Y_{ij} has independent increments given any nonoverlap pairwise time intervals. Thus, we denote $\Delta y_{ii} = y_{ii} - y_{i,i-1}$ the degradation increment from $t_{i,j-1}$ to t_{ij} . In addition, let $\omega_{ij} =$ $\Lambda(t_{ij}; \gamma_i) - \Lambda(t_{i,i-1}; \gamma_i)$ be the transformed inspection time interval, where $\Lambda(t_{ii}; \gamma_i)$ is a function to transform time scale if nonlinearity in the degradation process exists. Possible choices of $\Lambda(\cdot)$ include the power law function and the exponential law function (Whitmore & Schenkelberg, 1997). Under a Wiener process model, it is assumed that $\Delta Y_{ii} \sim N(\mu_i \omega_{ii}, \sigma_i^2 \omega_{ii})$, where $\mu_i \in \mathbb{R}$ is the location parameter and $\sigma_i^2 > 0$ is the scale parameter. Under a gamma process model, the MDP is modeled as $\Delta Y_{ii} \sim Ga(\alpha_i \omega_{ii}, \beta_i)$, where $\alpha_i > 0$ is the shape parameter and $\beta_i > 0$ is the rate parameter. Finally, for an IG process model, the degradation increment is subject to an IG distribution as $\Delta Y_{ij} \sim IG(\mu_i \omega_{ij}, \lambda_i \omega_{ij}^2)$, where $\mu_i > 0$ is the mean and $\lambda_i > 0$ is the shape parameter. For details about a number of variants of these models, please refer to (Lawless & Crowder, 2004; Li, Pan, & Chen, 2014; Ye & Chen, 2014; Ye et al., 2013). The two sets of Eqs. (8) and (9) demonstrate the pdfs and cdfs of the models, respectively.

$$f_{i}(\Delta y_{ij}) = \begin{cases} \frac{1}{\sqrt{2\pi\sigma_{i}^{2}\omega_{ij}}} \exp\left[-\frac{\left(\Delta y_{ij} - \mu_{i}\omega_{ij}\right)^{2}}{2\sigma_{i}^{2}\omega_{ij}}\right] & \text{for Wiener process} \\ \frac{\beta_{i}^{a_{i}\omega_{ij}}}{\Gamma(a_{i}\omega_{ij})} \Delta y_{ij}^{a_{i}\omega_{ij}-1} \exp(-\beta_{i}\Delta y_{ij}) & \text{for Gamma process} \end{cases} \tag{8} \\ \sqrt{\frac{\lambda_{i}\omega_{ij}^{2}}{2\pi\Delta y_{ij}^{3}}} \exp\left[\frac{-\lambda_{i}(\Delta y_{ij} - \mu_{i}\omega_{ij})^{2}}{2\mu_{i}^{2}\Delta y_{ij}}\right] & \text{for IG process.} \end{cases}$$

$$F_{i}(\Delta y_{ij}) = \begin{cases} \Phi\left(\frac{\Delta y_{ij} - \mu_{i}\omega_{ij}}{\sigma_{i}\sqrt{\omega_{ij}}}\right) & \text{for Wiener process} \\ \frac{\gamma(\alpha_{i}\omega_{ij}, \beta_{i}\Delta y_{ij})}{\Gamma(\alpha_{i}\omega_{ij})} & \text{for Gamma process} \end{cases}$$

$$F_{i}(\Delta y_{ij}) = \begin{cases} \Phi\left(\frac{\lambda_{ij}}{\sigma_{i}\sqrt{\omega_{ij}}}\right) & \text{for Gamma process} \\ \Phi\left[\sqrt{\frac{\lambda_{i}}{\Delta y_{ij}}}\left(\frac{\Delta y_{ij}}{\mu_{i}} - \omega_{ij}\right)\right] + \left(\exp\left(\frac{2\lambda_{i}\omega_{ij}}{\mu_{i}}\right)\Phi\left[-\sqrt{\frac{\lambda_{i}}{\Delta y_{ij}}}\left(\frac{\Delta y_{ij}}{\mu_{i}} + \omega_{ij}\right)\right] & \text{for IG process.} \end{cases}$$

3.2. Copula-based joint model

Based on the aforementioned MDP and multivariate copula models, a very natural and flexible way to construct a joint distribution model of dependent degradation processes is demonstrated as below:

$$\begin{cases}
F(\Delta Y_{1j}, \Delta Y_{2j}, ..., \Delta Y_{dj}) = C(F_1(\Delta y_{1j}), F_2(\Delta y_{2j}), ..., F_d(\Delta y_{dj}); \boldsymbol{\theta}^{Cop}) \\
\Delta Y_{ij} \sim MDP(\Delta y_{ij}; \boldsymbol{\theta}_i^{Mar}),
\end{cases}$$
(10)

where θ^{Cop} is the set of parameters in the copula function and θ_i^{Mar} is the set of parameters in the *i*-th MDP model. Under this framework, the copula function, $C(\cdot)$, can be any one of ECs, EACs, and VCs introduced before. The model of a MDP can be any one of the Wiener process, gamma process, or IG process described above. This joint model also covers the special case of independent degradation processes by assuming an independence copula. As implied by Model (10), the copula function indeed provides a way to construct a joint distribution function that makes all marginal models defined with no restriction; and the

dependence structure is built into the copula function separately from those marginals. In addition, it is noted that a lot of traditional multivariate model construction methods assume a Gaussian dependence structure, which is represented by the Gaussian copula or Student's *t* copula inherently. Such an example is the Nataf transformation (Lebrun & Dutfoy, 2009; Noh, Choi, & Du, 2007). But as explained in the introduction section, the Gaussian dependence structure cannot capture the nonlinear dependency or the tail dependency that may exist among the dependent degradation processes (Wang & Li, 2017). In later sections, we will evaluate the effect of model misspecification.

4. Reliability evaluation and RUL prediction

In this section, we provide the applications of the proposed methodology, including system reliability evaluation and RUL prediction.

4.1. Reliability evaluation

For an individual degradation process, $\{Y_i(t), t \geqslant 0\}$, the associated reliability is defined by the probability that the degradation value first passes a "soft" failure threshold \mathcal{D}_i within time t. Without loss of generality, we assume $Y_i(0) = 0$ and each PC increases up to \mathcal{D}_i until failure. Also, since most degradation processes are monotone, the marginal reliability can be defined by $R_i(t) = P(Y_i(t) < \mathcal{D}_i)$, which is simply the corresponding $\mathrm{cdf}\, F_i(\mathcal{D}_i)$ for MDP i in Eq. (9). Thus, the system reliability for a series system is

$$\begin{array}{ll} R_{sys}(t) = & P(Y_1(t) < \mathcal{D}_1, Y_2(t) < \mathcal{D}_2, ..., Y_d(t) < \mathcal{D}_d) \\ = & C(R_1(t), R_2(t), ..., R_d(t)), \end{array}$$

which is the copula function with entries $R_i(t)$, i=1,2,...,d, in Eq. (10). For a parallel system, the system reliability is

$$R_{sys}(t) = 1 - P(Y_1(t) \geqslant D_1, Y_2(t) \geqslant D_2, ..., Y_d(t) \geqslant D_d) = 1 - \overline{C}(1 - R_1(t), 1 - R_2(t), ..., 1 - R_d(t)),$$

where $\overline{C}(\cdot)$ is the survival copula provided in Table 3.

Remark:. If a degradation process is not monotone, the Wiener process is often utilized as a MDP model. In such case, the marginal reliability equals to the cdf of a derived IG distribution (Whitmore & Seshadri, 1987).

4.2. RUL prediction

For online monitoring purpose, the RUL prediction is often carried out. When a system with d dependent competing degradation processes is monitored up to time t and no failure is observed, the RUL is defined by

$$\text{RUL} = \inf \left\{ \begin{array}{ll} Y_1(t+\tau) {\geqslant} \mathcal{D}_1 & y_1(t) < \mathcal{D}_1 \\ \text{or} & \text{and} \\ \tau : & \vdots & \vdots \\ \text{or} & \text{and} \\ Y_d(t+\tau) {\geqslant} \mathcal{D}_d & y_d(t) < \mathcal{D}_d \end{array} \right\},$$

for which it is difficult to find the analytical solution. Instead, we utilize a simulation-based method to make RUL prediction. Suppose the degradation observations up to time point j is denoted by $\{y_{1:d,1},...,y_{1:d,j}\}$, where $y_{1:d,j}=(y_{1j},y_{2j},...,y_{dj})^{'}$ is the vector of observations at time point j. With all the available data, the estimated parameters $-\widehat{\theta}^{Cop}$ and $\widehat{\theta}^{Mar}_{1:d}$ for both the copula function and the marginal models – can be easily obtained. Then, a group of random samples, $(u_1,...,u_d)$, are generated from the copula function, $C(u_1,...,u_d;\widehat{\theta}^{Cop})$. By utilizing the inverse cdf technique, $F_i^{-1}(u_i;\widehat{\theta}^{Mar}_i)$, the degradation increment for a specified time interval Δt is acquired for each MDP. Finally, the

predicted degradation level is obtained by adding the corresponding increment to the current degradation level. This process is continued until any MDP passes its failure threshold. In summary, the simulation-based RUL prediction is given by Algorithm 1. By repeating the algorithm for a large amount of repetitions, say B = 1,000, a group of RULs are obtained and a statistical summary can be carried out.

Algorithm 1. RUL Prediction for Series Systems

```
Data: \{y_{1:d,j}\}, \{\hat{\boldsymbol{\theta}}^{Cop}, \hat{\boldsymbol{\theta}}^{Mar}_{1:d}\}, \text{ and } \Delta t

Result: RUL

RUL=0 and \hat{\boldsymbol{y}}_{1:d} = \boldsymbol{y}_{1:d,j};

while \hat{y}_1 < \mathcal{D}_1 \& \cdots \& \hat{y}_d < \mathcal{D}_d do

RUL=RUL+\Delta t;

Generate (u_1, \dots, u_d) from C(u_1, \dots, u_d; \hat{\boldsymbol{\theta}}^{Cop});

for i=1:d do

\hat{y}_i = \hat{y}_i + F_i^{-1}(u_i; \boldsymbol{\theta}_i^{\hat{M}ar});

end

end
```

Algorithm 2. Sampling Algorithm For VCs (Czado, 2019)

```
\begin{array}{l} \textbf{Input: Sample } \textit{w}_{i} \overset{i.i.d.}{\sim} \textit{Unif}(0,1), i = 1,2,...,d. \\ \textbf{Output: } \textit{u}_{1} := \textit{w}_{1} \\ & \textit{u}_{2} := \textit{C}_{2|1}^{-1}(\textit{w}_{2} \middle| \textit{u}_{1}) \\ & \vdots \\ & \textit{u}_{d} := \textit{C}_{d|d-1,...,1}^{-1}(\textit{w}_{d} \middle| \textit{u}_{d-1},...,\textit{u}_{1}) \end{array}
```

Note that in Algorithm 1 a sampling process to generate random samples from the copula function is involved. This procedure is straightforward for ECs and EACs due to the feature that all marginals are integrated in a single joint cdf. However, for VCs, this is not the case. To draw a sample from a *d*-dimensional VC, the general algorithm based on the following stepwise inverse transformation method is needed (Algorithm 2). In Algorithm 2, the existing results on Table 5 together with the relation about the variables implied by the vine structure are useful to calculate the conditional cdfs. We will use examples to illustrate how to apply this algorithm in Section 6.1.

Remark: For parallel systems, the RUL becomes

$$\text{RUL} = \inf \left\{ \begin{array}{ll} Y_1(t+\tau) \geqslant \mathcal{D}_1 & y_1(t) < \mathcal{D}_1 \\ \text{and} & \text{or} \\ \tau : & \vdots \\ \text{and} & \text{or} \\ Y_d(t+\tau) \geqslant \mathcal{D}_d & y_d(t) < \mathcal{D}_d \end{array} \right\}$$

and the condition in the while loop in Algorithm 1 becomes $\widehat{y}_1 < \mathcal{D}_1 \mid \cdots \mid \widehat{y}_d < \mathcal{D}_d$.

5. Statistical inference and model selection

In this section, we provide a statistical inference method and a tailored workflow of model selection, including two graphical diagnostic tools, a test of independence and a GOF test.

5.1. Statistical inference

As implied by Eq. (1), the joint pdf of observed degradation increments at time point j is given by

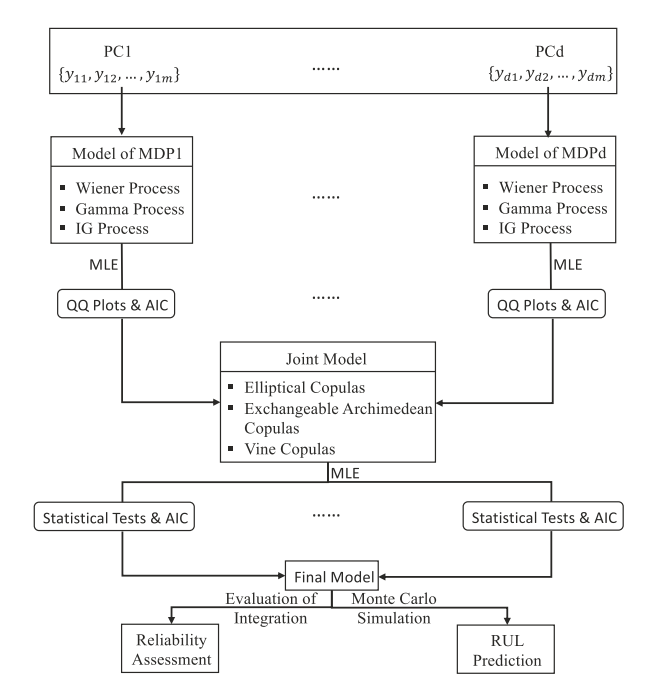


Fig. 3. Flowchart of Copula-based Degradation Data Analysis.

$$f(\Delta y_{1j}, \Delta y_{2j}, ..., \Delta y_{dj}) = c(F_1(\Delta y_{1j}), F_2(\Delta y_{2j}), ..., F_d(\Delta y_{dj})) \prod_{i=1}^d f_i(\Delta y_{ij}).$$

Suppose the degradation increments for all processes up to termination time are denoted by $\Delta y_{1:d} = \{\Delta y_1, \ \Delta y_2, \ ..., \ \Delta y_d\}$, where $\Delta y_i = (\Delta y_{i1}, \Delta y_{i2}, ..., \Delta y_{im})'$. Thus, the log-likelihood function is given by

$$\ln L(\boldsymbol{\theta}^{Cop}, \boldsymbol{\theta}_{1:d}^{Mar} | \Delta \mathbf{y}_{1:d}) \\
= \sum_{j=1}^{m} \ln c(F_1(\Delta \mathbf{y}_{1j}), F_2(\Delta \mathbf{y}_{2j}), ..., F_d(\Delta \mathbf{y}_{dj}) | \boldsymbol{\theta}^{Cop}) + \sum_{i=1}^{d} \sum_{j=1}^{m} \ln f_i(\Delta \mathbf{y}_{ij} | \boldsymbol{\theta}_i^{Mar}). \tag{11}$$

Obviously, it is potentially difficult and also computationally expensive to infer the unknown parameters by performing maximum likelihood estimation (MLE) on the whole log-likelihood function directly. Instead, a popular two-stage inference method, inference function for margins (IFM) (Joe, 2005), is available to reduce the computational burden. As illustrated by Peng et al. (2016) Sun et al. (2020),ang et al. (2020) already, this method also has satisfactory asymptotic efficiency for both estimating the parameters of copula-based degradation models and making RUL predictions. Thus, we employ the IFM, which has the following two steps:

1. Perform MLE for individual marginal models:

$$\widehat{\boldsymbol{\theta}}_{i}^{Mar} = \operatorname{argmax}_{\boldsymbol{\theta}_{i}^{Mar}} \sum_{j=1}^{m} \ln f_{i}(\Delta y_{ij} \middle| \boldsymbol{\theta}_{i}^{Mar}) \ \forall i = 1, 2, ..., d;$$

2. Perform MLE for the copula model:

$$\widehat{\boldsymbol{\theta}}^{Cop} = \operatorname{argmax}_{\boldsymbol{\theta}^{Cop}} \sum_{j=1}^{m} \operatorname{lnc}(\widehat{F}_{1}(\Delta y_{1j}), \widehat{F}_{2}(\Delta y_{2j}), ..., \widehat{F}_{d}(\Delta y_{dj}) \middle| \boldsymbol{\theta}^{Cop}).$$

In the second step, $\hat{F}_i(\Delta y_{ij})$, i = 1, 2, ..., d, is the estimated marginal

cdf, of which the estimated parameters $\widehat{\theta}_i^{Mar}$ comes from step 1. Intuitively, one can view $\widehat{F}_i(\Delta y_{ij})$ as the pseudo-observation from the copula model. And the density for various copula functions is available in Table 5.

5.2. Model selection

Based on the method of parameters estimation introduced above, two graphical diagnostic methods, a test of independence, and a GOF test are used to help search the best model among candidate models.

Suppose after step 1 in the IFM, given all candidate marginal models with estimated parameters for MDPs, we select the best fitted model based on both the quantile-quantile (QQ) plot and the Akaike Information Criterion (AIC). The AIC value is defined by AIC = $2(p-\ln \hat{L})$, where p is the total number of parameters and \hat{L} is the value of the likelihood function for the fitted model. Given two candidate models, the preferred model is the one with lower AIC value. For the three marginal degradation models, we utilize the corresponding QQ plots shown as below:

1. Wiener process: Standard Normal QQ plot

Theorem: If $X \sim N(\mu, \sigma^2)$, then $\frac{X-\mu}{\sigma} \sim N(0, 1)$. Result: For the Wiener process, $\Delta Y_{ij} \sim N(\mu \omega_{ij}, \sigma^2 \omega_{ij})$, j=1,2,...,m, $\forall i=1,2,...,d$, the resulted statistics $\frac{\Delta y_{ij} - \widehat{\mu} \omega_{ij}}{\sigma \sqrt{\omega_{ij}}} \overset{i.i.d.}{\sim} N(0,1)$.

2. Gamma process: Standard Normal QQ plot

Theorem: If
$$X \sim Ga(\alpha, \beta)$$
, then $\sqrt[3]{\frac{\beta X}{\alpha}} \stackrel{approx.}{\sim} N(1 - \frac{1}{9\alpha}, \frac{1}{9\alpha})$. Thus, $3\sqrt{\alpha} \left[\sqrt[3]{\frac{\beta X}{\alpha}} - 1 + \frac{1}{9\alpha} \right] \sim N(0, 1)$.

Result: For the gamma process, $\Delta Y_{ij} \sim Ga(\alpha\omega_{ij},\beta), j=1,2,...,m, \ \forall i=1,2,...,d,$ the resulted statistics $3\sqrt{\alpha\omega_{ij}}\left[\sqrt[3]{\frac{\beta\Delta Y_{ij}}{\alpha\omega_{ij}}}-1+\frac{1}{9\alpha\omega_{ij}}\right]^{i.i.d.}N(0,$

1).

3. IG process: Chi-square QQ plot

Theorem: If $X \sim IG(\mu,\lambda)$, then $\frac{\lambda(X-\mu)^2}{\mu^2 X} \sim \chi_1^2$. Result: For the IG process, $\Delta Y_{ij} \sim IG\Big(\mu\omega_{ij},\lambda\omega_{ij}^2\Big), j=1,2,...,m, \ \forall i=1,2,...,d$, the resulted statistics $\frac{\widehat{\lambda}(\Delta y_{ij}-\widehat{\mu}\omega_{ij})^2}{\widehat{\mu}^2 \Delta y_{ij}} \overset{i.i.d.}{\sim} \chi_1^2$.

After finding the best fitted models for MDPs, a scatter plot of all bivariate margins, i.e. pseudo-observations, can be generated to visualize dependence patterns. A rough appearance of potential correlation and/or tail-dependence if existing would be suggested by this graphical diagnostic plot. Then, to formally test the dependence among the MDPs, we make use of a test of independence that is explained by Genest and Rémillard (2004) and Genest, Quessy, and Rémillard (2007). If the test result shows statistically independence, the degradation processes can be treated independently. Otherwise, we proceed to the step of joint model fitting, where ECs, EACs, and VCs are considered. To carry out the GOF test, we utilize a "blanket test" that is based on the empirical copula (Genest, Rémillard, & Beaudoin, 2009). After this step, acceptable parametric copula models are narrowed down and the AIC values can be compared to finally select the best joint degradation model. Specifically, the test of independence and the GOF test are given as follows:

1. The test of independence

Hypothesis: $\mathcal{H}_0: C = \Pi$ versus $\mathcal{H}_1: C \neq \Pi$, Test statistic:

$$S_m^{\Pi} = \int_{[0,1]^d} m(C_n(\boldsymbol{u}) - \Pi(\boldsymbol{u}))^2 d\boldsymbol{u}$$

=
$$\sum_{j=1}^m \left(C_n(\boldsymbol{U}_{j,m}) - \Pi(\boldsymbol{U}_{j,m}) \right)^2,$$

Approximate p-value: $rac{1}{N+1} igg(\sum_{k=1}^N \mathbf{1} \Big(S_m^{\Pi,(k)} \geq S_m^\Pi \Big) + rac{1}{2} igg)$

2. The GOF test

Hypothesis: $\mathcal{H}_0: C \in \mathcal{C}$ versus $\mathcal{H}_1: C \notin \mathcal{C}$, Test statistic:

$$S_m^{\text{gof}} = \int_{[0,1]^d} m(C_n(\boldsymbol{u}) - C_{\boldsymbol{\theta}_m}(\boldsymbol{u}))^2 dC_n(\boldsymbol{u})$$

$$= \sum_{i=1}^m (C_n(\boldsymbol{U}_{j,m}) - C_{\boldsymbol{\theta}_m}(\boldsymbol{U}_{j,m}))^2,$$

Approximate
$$p$$
-value: $\frac{1}{N+1}\left(\sum_{k=1}^{N}\mathbf{1}\left(S_{m}^{\mathrm{gof},(k)}\geq S_{m}^{\mathrm{gof}}\right)+\frac{1}{2}\right)$

Remark: (1) The construction of the QQ plot for the Wiener process is straightforward, while the methods to build QQ plots for both the gamma process and the IG process are adopted from Wang and Xu (2010)'s work (Wang & Xu, 2010). (2) The test of independence is to assess whether the copula model C is different from the independence copula Π. The GOF test is to assess whether the copula model C belongs to a copula family C. (3) $C_{\theta_m}(\cdot)$ is the parametric copula of interest. And $C_n(u)$ is the nonparametric copula defined by

$$C_n(\boldsymbol{u}) = \frac{1}{m} \sum_{j=1}^m \mathbf{1} \big(U_{j,m} \leqslant \boldsymbol{u} \big) = \frac{1}{m} \sum_{j=1}^m \prod_{i=1}^d \mathbf{1} \Big(\widehat{F}_i(\Delta y_{ij}) \leqslant u_i \Big), \boldsymbol{u} \in [0,1]^d,$$

where $U_{j,m}=(\widehat{F}_1(\Delta y_{1j}),\widehat{F}_2(\Delta y_{2j}),...,\widehat{F}_d(\Delta y_{dj})), j=1,2,...,m$, are the pseudo-observations and $U_{j,m} \leqslant u, j=1,2,...,m$, is a component-wise inequality. The use of the nonparametric copula is based on the conclusion that it is a consistent estimator of the parametric copula (Segers, 2012). Both test statistics are based on the Cramer-von Mises statistic. (4) The approximate p-value is computed using a bootstrap algorithm, where N is the total number of simulations. See (Genest & Rémillard, 2004; Genest & Rémillard, 2008) for more details about the algorithm. (5) These two tests are adopted in two R packages – copula and VineCopula (a continuing version of the package CDVine) (Brechmann & Schepsmeier, 2013; Yan, 2007).

In order to briefly summarize the methodology introduced above, Fig. 3 presents a flowchart of copula-based degradation data analysis.

6. Simulation study

In this section, we carry out three Monte Carlo simulation experiments to illustrate the characteristics of the introduced multivariate copula models and the characteristics of the proposed multivariate degradation models, and to provide a discussion on model misspecification.

6.1. Characteristics of multivariate copula models

In Section 2, three fundamental classes of copula models – ECs, EACs, and VCs – are introduced. To demonstrate their characteristics, we simulate data from three trivariate models with a Gaussian copula, an exchangeable Gumbel copula, and a D-vine, respectively. For the Gaussian copula, we assume the pairwise Pearson correlations are $\rho_{12}=0.2, \rho_{23}=0.5$, and $\rho_{13}=0.8$. For the exchangeable Gumbel copula, we use the association parameter $\delta=3$. For the D-vine, we assume the joint pdf is defined by Eq. (7), which covers $C_{1,2}$ – the Student's t copula with

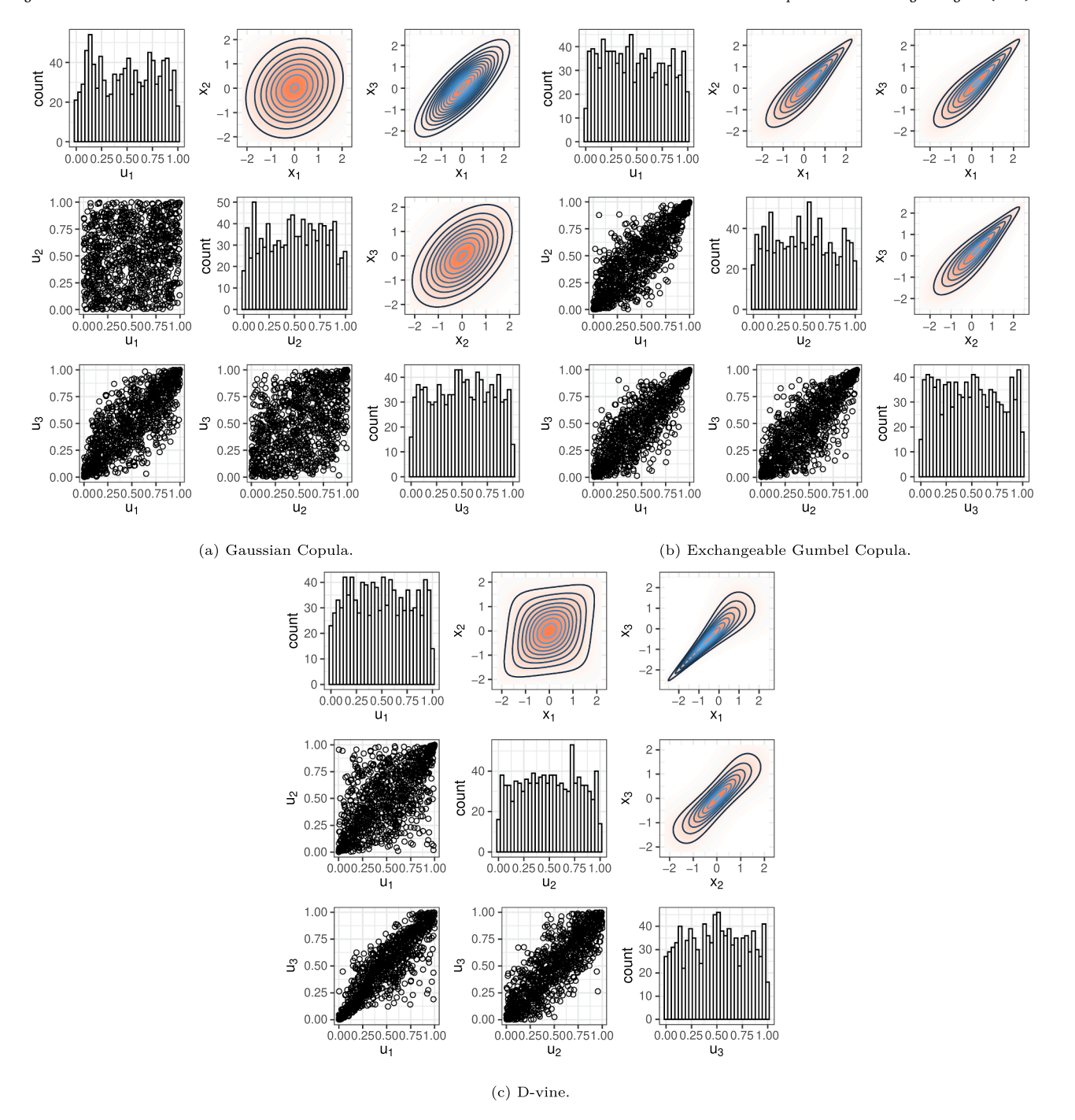


Fig. 4. Histograms, Scatter Plots, and Contour & Density Plots of Simulation Models.

 $\nu=3$ and $\rho_{12}=0.7, C_{2,3}$ – the Frank copula with $\delta=10$, and $C_{1,3|2}$ – the Clayton copula with $\delta=4$. For each model, 1,000 random vectors (i.e. $(u_1,u_2,u_3)^{'}$) are generated. Following Algorithm 2, the specific steps to simulate data from a 3-dimensional D-vine are given as follows:

- 1. Sample $w_i^{i.i.d.}$ Unif (0,1), i = 1,2,3;
- 2. $u_1 := w_1$;
- 3. $u_2:=C_{2|1}^{-1}(w_2|u_1)$, where $C_{2|1}^{-1}(w_2|u_1)$ is the inverse function of $C_{2|1}(w_2|u_1)=\frac{\partial C_{1,2}(u_1,w_2)}{\partial u_1}$.

This is equivalent to $u_2:=h_{2|1}^{-1}(w_2|u_1;\theta_{12})$, where θ_{12} is the parameters embedded in $C_{1,2}$;

4. $u_3:=C_{3|1,2}^{-1}(w_3|u_1,u_2)$, where $C_{3|1,2}^{-1}(w_3|u_1,u_2)$ is the inverse function of $C_{3|1,2}(w_3|u_1,u_2)=\frac{\partial C_{1,3|2}(F_{3|2}(w_3|u_2),F_{1|2}(u_1|u_2))}{\partial F_{1|2}(u_1|u_2)}$ with $F_{3|2}(w_3|u_2)=\frac{\partial C_{2,3}(u_2,w_3)}{\partial u_2}$ and $F_{1|2}(u_1|u_2)=\frac{\partial C_{1,2}(u_1,u_2)}{\partial u_2}$. This is equivalent to

$$u_3 := h_{3|2}^{-1} \Big(h_{3|1,2}^{-1} \big(w_3 \big| h_{1|2} \big(u_1 \big| u_2, \boldsymbol{\theta}_{12} \big), \boldsymbol{\theta}_{13|2} \big) \Big| u_2, \boldsymbol{\theta}_{23} \Big),$$

where θ_{13} and $\theta_{13|2}$ are the parameters embedded in $C_{1,3}$ and $C_{1,3|2}$, respectively.

Fig. 4 illustrates relevant plots generated from the simulation models. These plots include histograms and scatter plots of simulated data with uniform margins, along with contour & density plots of the

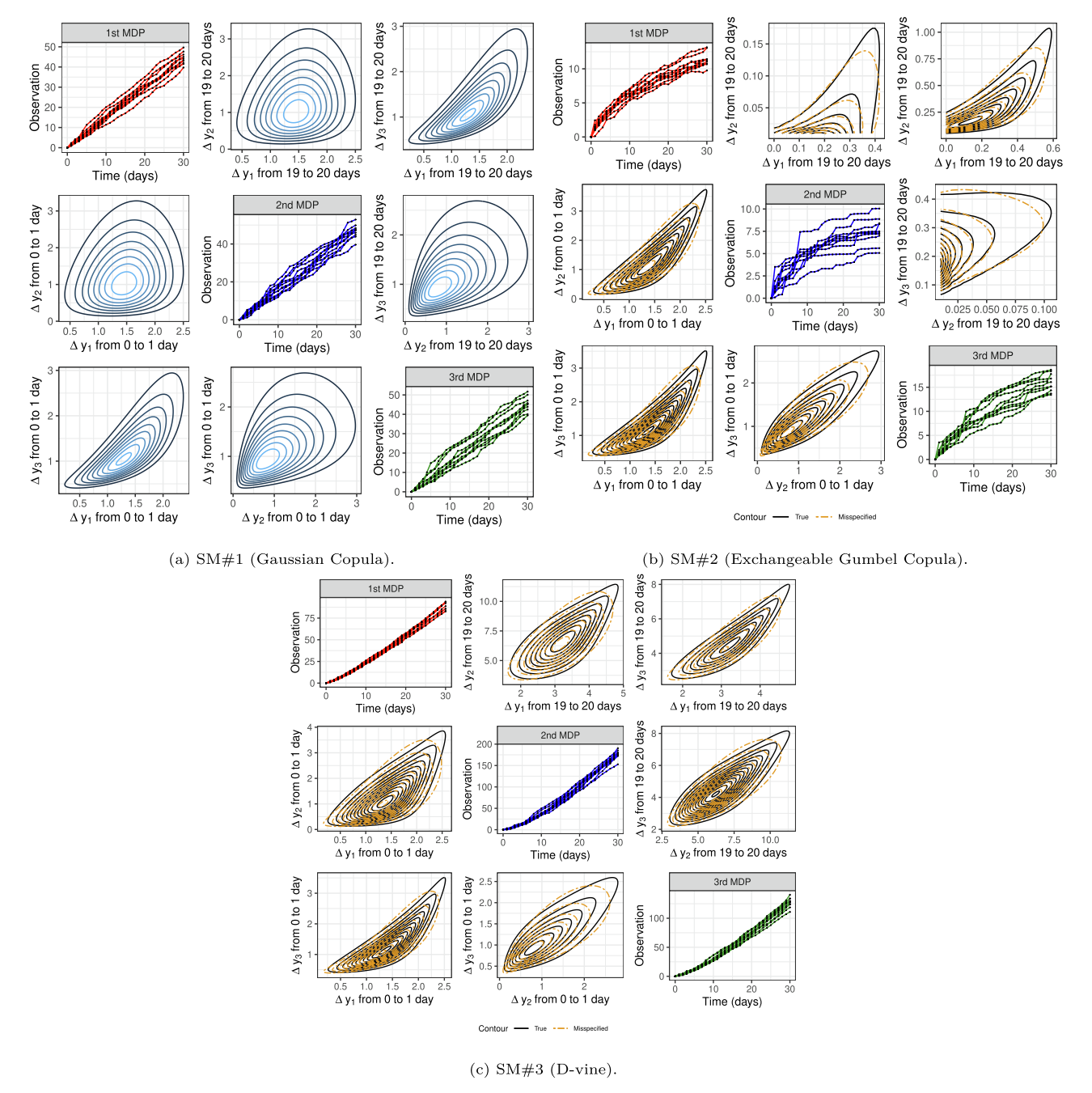


Fig. 5. Degradation Paths and Contour & Density Plots of Simulation Models.

simulation models with standard normal margins. It can be seen that the Gaussian copula, originated from the multivariate normal distribution, presents the symmetric feature with no tail dependence. And the magnitude of dependence among margins is controlled by the value of the Pearson correlation. On the other hand, the exchangeable Gumbel copula demonstrates asymmetric feature with strong upper-tail dependence, but the degree of dependence is the same across all pairs of variables. This is because EACs use a single association parameter to specify pairwise dependence, which actually indicates the exchangeability. Thus, ECs and EACs, to some extent, are restrictive models. In contrast, Plot Fig. 4c shows that both symmetric and asymmetric feature are available in the D-vine and the degree of dependence varies pair by pair. Thus, VCs are very flexible since each pairwise relationship can be

described by any freely-chosen bivariate copula.

Remark:. For $C_{1,3|2}(u_1, u_3|u_2)$, we make the so-called simplifying assumption (Killiches, Kraus, & Czado, 2017), i.e. $C_{1,3|2}(u_1,u_3|u_2) = C_{1,3|2}(u_1,u_3)$, to enable visualizing the contour & density plot between x_1 and x_3 .

6.2. Characteristics of multivariate degradation models

Next, we study characteristics of the proposed copula-based multivariate degradation models. To do that, three simulation models – SM#1, SM#2, and SM#3 – are presented as below:

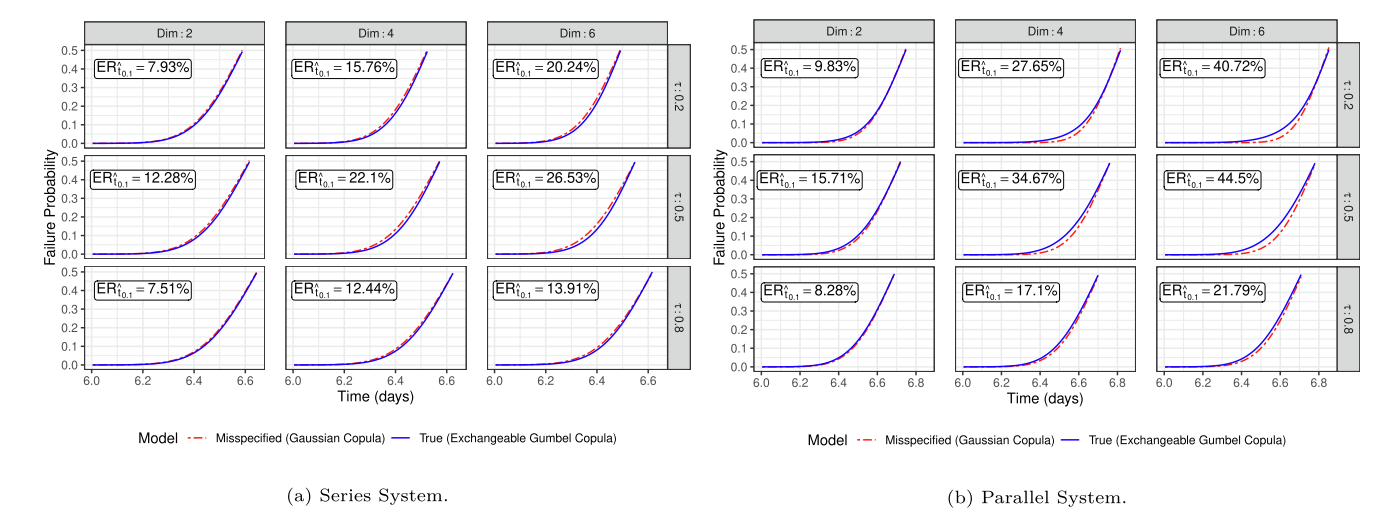


Fig. 6. Failure Probability Curves at Early Stage.

$$SM\#1: \begin{cases} F(\Delta y_{1j}, \Delta y_{2j}, \Delta y_{3j}) = \Phi_{\Sigma}(\Phi^{-1}(F_1(\Delta y_{1j})), \Phi^{-1}(F_2(\Delta y_{2j})), \Phi^{-1}(F_3(\Delta y_{3j}))) \\ \Delta Y_{1j} \sim N(1.5\omega_{1j}, 0.5^2\omega_{1j}), \omega_{1j} = t_j - t_{j-1} \\ \Delta Y_{2j} \sim Ga(3\omega_{2j}, 2), \omega_{2j} = t_j - t_{j-1} \\ \Delta Y_{3j} \sim IG(1.5\omega_{3j}, 6\omega_{3j}^2), \omega_{3j} = t_j - t_{j-1}. \end{cases}$$

$$SM\#2: \begin{cases} AY_{1j}, \Delta y_{2j}, \Delta y_{3j}) - C_{Glumbel}(F_1(\Delta y_{1j}), F_2(\Delta y_{2j}), F_3(\Delta y_{3j}), ... \\ \Delta Y_{1j} \sim N\left(1.5\omega_{1j}, 0.5^2\omega_{1j}\right), \omega_{1j} = t_j^{0.6} - t_{j-1}^{0.6} \\ \Delta Y_{2j} \sim Ga\left(3\omega_{2j}, 2\right), \omega_{2j} = t_j^{0.5} - t_{j-1}^{0.5} \\ \Delta Y_{3j} \sim IG\left(1.5\omega_{3j}, 6\omega_{3j}^2\right), \omega_{3j} = t_j^{0.7} - t_{j-1}^{0.7}. \end{cases}$$

$$\begin{cases} f\left(\Delta y_{1j}, \Delta y_{2j}, \Delta y_{3j}\right) = f_1\left(\Delta y_{1j}\right) \cdot f_2\left(\Delta y_{2j}\right) \cdot f_3\left(\Delta y_{3j}\right) \cdot \\ c_{1,2}\left(F_1\left(\Delta y_{1j}\right), F_2\left(\Delta y_{2j}\right)\right) \cdot c_{2,3}\left(F_2\left(\Delta y_{2j}\right), F_3\left(\Delta y_{3j}\right)\right) \cdot \\ c_{1,3|2}\left(F_{1|2}\left(\Delta y_{1j}|\Delta y_{2j}\right), F_{3|2}\left(\Delta y_{3j}|\Delta y_{2j}\right)\right) \\ \Delta Y_{1j} \sim N\left(1.5\omega_{1j}, 0.5^2\omega_{1j}\right), \omega_{1j} = t_j^{1.2} - t_{j-1}^{1.2} \\ \Delta Y_{2j} \sim Ga\left(3\omega_{2j}, 2\right), \omega_{2j} = t_j^{1.4} - t_{j-1}^{1.4} \\ \Delta Y_{3j} \sim IG\left(1.5\omega_{3j}, 6\omega_{3j}^2\right), \omega_{3j} = t_j^{1.3} - t_{j-1}^{1.3}. \end{cases}$$

In each model, three streams of degradation data are simulated. Among them, SM#1 assumes a Gaussian copula on modeling the joint distribution with the Pearson correlations – $\rho_{12}=0.2, \rho_{23}=0.5,$ and $\rho_{13}=0.8.$ SM#2 covers an exchangeable Gumbel copula with $\delta=3$, while SM#3 is characterized by a D-vine. For the pair copulas in SM#3, we assume $C_{1,2}, C_{2,3}$, and $C_{1,3|2}$ are all a bivariate Gumbel copula with $\delta_{12}=2,\delta_{23}=2.5,$ and $\delta_{13|2}=3,$ respectively. The reason of choosing the Gumbel copula is that upper-tail dependence is commonly seen in dependent degradation processes. We will explain more about this point later.

For all models, the three MDPs are separately characterized by the Wiener process, gamma process, and IG process, where the associated parameters are given in numbers on the model equations. And we as-

sume the degradation evolves in units of days. To reduce the bias caused by simulation, a total of 30 observations with $\Delta t=1$ are generated and we repeat this process for 10 times for each model. Note that to simulate degradation increments, it is only needed to apply the inverse cdf method by $F_i^{-1}(u_i)$, where $F_i(\cdot)$ is the cdf of the corresponding MDP model. Moreover, for SM#2 and SM#3, instead of the actual exchangeable Gumbel copula and D-vine, a Gaussian copula as an approximation is selected to model the multivariate joint distribution. Fig. 5 presents the simulation result of each model on separate plots. In each plot, we illustrate the degradation paths of each MDP and the contour & density plots in two different time phases. Particularly, on Plots Figs. 5b and c, we also draw the contour lines of the Gaussian copula using orange dashed lines. From these studies the following conclusions can be drawn.

First of all, as reasoned in Section 6.1, SM#3 is the most flexible model. Comparing with SM#1, there exists upper-tail dependence for each pair of MDPs. Comparing with SM#2, it reflects diverse magnitude of dependence. Thus, the VC is a good tool to model dependent degradation processes.

Secondly, it is easy to see that the copula-based multivariate degradation models are capable to incorporate any type of marginal degradation models. This is an advantage comparing with the aforementioned two traditional multivariate degradation models – the multivariate general path model (Si, Yang, Wu, & Chen, 2018) and multivariate Wiener process model (Wang et al., 2015); because these two models are essentially based on the multivariate normal distribution, of which marginal models are normal distribution.

Thirdly, the copula-based multivariate degradation models combined with the stochastic process models as marginals are able to present the dynamics of the degradation process. That is, when the parameter of the time scale transformation $\gamma=1$, the contour & density plot remains identical in the two phases. This is because the degradation rate doesn't change over time. However, if $\gamma\neq 1$, the contour & density plot varies

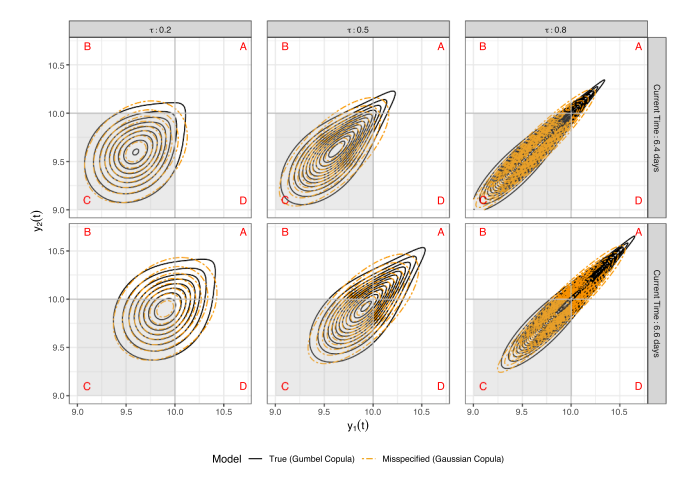


Fig. 7. Contour Plots for Study of Model Misspecification.

phase by phase due to either the concavity or convexity of the mean degradation function. These phenomena have been explored by Fang et al. (2020).

Lastly, and most importantly, it is noticed that if the Gaussian copula is chosen as *priori*, the resulted joint density will be inconsistent with the true density. As shown by Plots Figs. 5b and c, it can be seen that the Gaussian copula attempts to approximate the true model, but the contour plots resulted doesn't fully match the real ones and usually there is a non-overlapping area in the upper-tail part. This is due to the discrepancy in tail dependence between the Gaussian copula and the Gumbel copula. To evaluate the effect of ignoring the tail dependence, in the next part, we will carry out another simulation study.

6.3. Effect of model misspecification

In this part, we conduct the third simulation study to examine the effect of ignoring tail dependence on system failure probability assessment. For convenience, we assume a set of 2-, 4-, and 6-dimensional multivariate degradation processes are available with each MDP being subject to an identical Wiener process ($\mu = 1.5, \sigma = 0.1$, and $\gamma = 1$) and having the same failure threshold – $\mathcal{D}=10$. The exchangeable Gumbel copula is supposed to be the true model that governs each multivariate degradation process; and we set three levels of dependence – $\tau = 0.2$ (mild dependence), $\tau = 0.5$ (moderate dependence), and $\tau = 0.8$ (strong dependence). Thus, a total of 9 multivariate degradation processes with various dimensions (i.e. number of MDPs) and diverse magnitude of dependence are investigated. Meanwhile, we assume the Gaussian copula is assigned to model these processes too. Under such setting, both the true model and the misspecified model are fitted with the same MDP models and identical degree of dependence, where the Kendall's τ is converted to either the association parameter in the exchangeable Gumbel copula or the Pearson correlation in the Gaussian copula through the relationship between these measures provided in Table 4.

Considering the fact that the lower-tail failure time is of much interest in end use, we demonstrate the failure probability curves at early stage, during which the true failure probability $P_f^{\textit{True}} \leqslant 0.5$, to indicate the effect of model misspecification. Fig. 6 presents the results for both series systems and parallel systems, where failure probability is calculated according to the conclusions in Section 4.1 and evaluated at intervals of 0.004 time units. To assess the performance of the approximation to the true failure probability by the misspecified model, on each plot of Fig. 6, we also report a metric – error ratio at $\hat{t}_{0.1}$ (i.e. the estimated 10-th quantile failure time), which is defined by

$$ER_{\widehat{t}_{0.1}} = \frac{\left| P_f^{Misspecified} - P_f^{True} \right|}{P_f^{True}} \times 100\%,$$

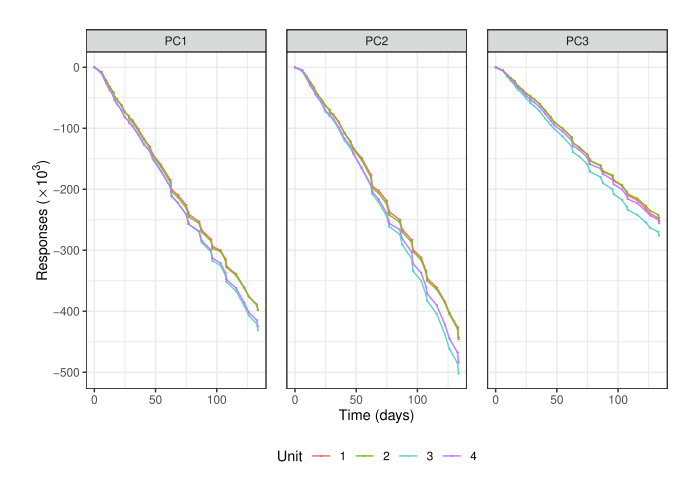


Fig. 8. Degradation Paths of Polymeric Materials.

where P_f^{True} and $P_f^{Misspecified}$ are failure probability at $\hat{t}_{0.1}$ for the true model and the misspecified model, respectively.

It is found that for all cases, the misspecified model overestimates failure probability for series systems at early stage, where the opposite is true for parallel systems. By looking at $ER_{\widehat{t}_{0,1}}$, the approximation error is relatively bigger for parallel systems. It is also noticed that under each setting of the Kendall's τ , the approximation error increases as the dimension becomes higher. On the other hand, under each setting of dimension, the approximation error is the biggest under moderate dependence. In order to explain these interesting findings, contour plots for both a bivariate Gumbel copula and a Gaussian copula are presented in Fig. 7. These contour plots indicate various equal-density lines under three levels of dependence at two different elapsed moments – t=6.4 and t=6.6 days. On each plot, contours for both the true model and the misspecified model are depicted in black solid lines and orange dashed lines, respectively.

First, as represented on each plot in Fig. 7, there exists a partially transparent grey area C, which is the projected area of the density surface cut by the two failure thresholds. And the volume under the joint pdf surface in this area is $P(Y_1(t) \le 10, Y_2(t) \le 10)$. Thus, for parallel systems, the failure probability, $P(Y_1(t) > 10, Y_2(t) > 10)$, corresponds to the volume under the joint pdf surface in area A. And for series systems, the failure probability, $1 - P(Y_1(t) < 10, Y_2(t) < 10)$, corresponds to the volume in the combined projected area A + B + D. Second, it is further noticed that the density of the Gumbel copula is concentrated in area A. On the contrary, the density surface of the Gaussian copula covers more in areas B and D. Due to this discrepancy in upper-tail dependence between the Gumbel copula and the Gaussian copula, it results in the phenomenon that the Gaussian copula underestimates failure probability for parallel systems. But for series systems, overestimation is expected because of extra volume provided by the Gaussian copula in areas B and D; and together with the addition of volume in area A, the approximation error is relatively smaller. With time elapsing, the magnitude of overestimation/underestimation develops as the coverage of the areas varies. In terms of the effect of the magnitude of dependence, one can see that the difference between the two models in contours is the most significant under moderate dependence. This is because the shape of the contours of the Gumbel copula is closer to ellipse under either mild or strong dependence, which makes the Gaussian copula an acceptable approximate. Last, it is easy to see that the approximation error would definitely increase as dimension becomes higher due to the accumulated error by more pairs of marginals. Thus, in summary, major concern should be given when applying the Gaussian copula arbitrarily in analyzing an upper-tail dependent high-dimensional multivariate degradation process with moderate dependence. And it is more serious for parallel systems.

Table 1Results of Parameters Estimation for MDPs.

Parameter	PC1	PC2	PC3
Wiener process			
μ	1.419	0.467	1.023
σ	3.274	2.036	2.168
γ	1.159	1.412	1.130
AIC	952.033	981.032	821.202
Gamma process			
α	0.904	0.434	0.970
β	0.281	0.250	0.505
γ	0.992	1.144	1.000
AIC	960.193	981.781	815.166
IG process			
$\frac{\mu}{\mu}$	3.498	1.896	2.024
λ	3.027	0.796	1.932
γ	0.975	1.126	0.990
AIC	978.167	993.900	828.449

Remark: For convenience, the study above is developed for the exchangeable Gumbel copula as the true model. It can be readily modified for the study for the flexible VC as the true model. To implement that, a R package – vinecopulib (Nagler & Vatter, 2019) – is needed to evaluate the joint cdf. Nevertheless, the conclusions above still hold.

7. Application

In this section, we use a numerical example to demonstrate the application of the proposed methodology. Motivated by the existing work of Lu et al. (2020), we revisit a degradation dataset of a type of polymeric material. This dataset presents the material's

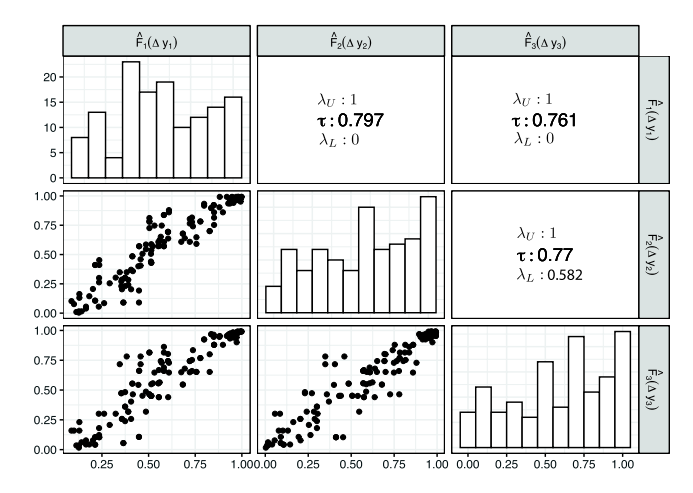


Fig. 10. Scatter Plot of Pseudo-observations.

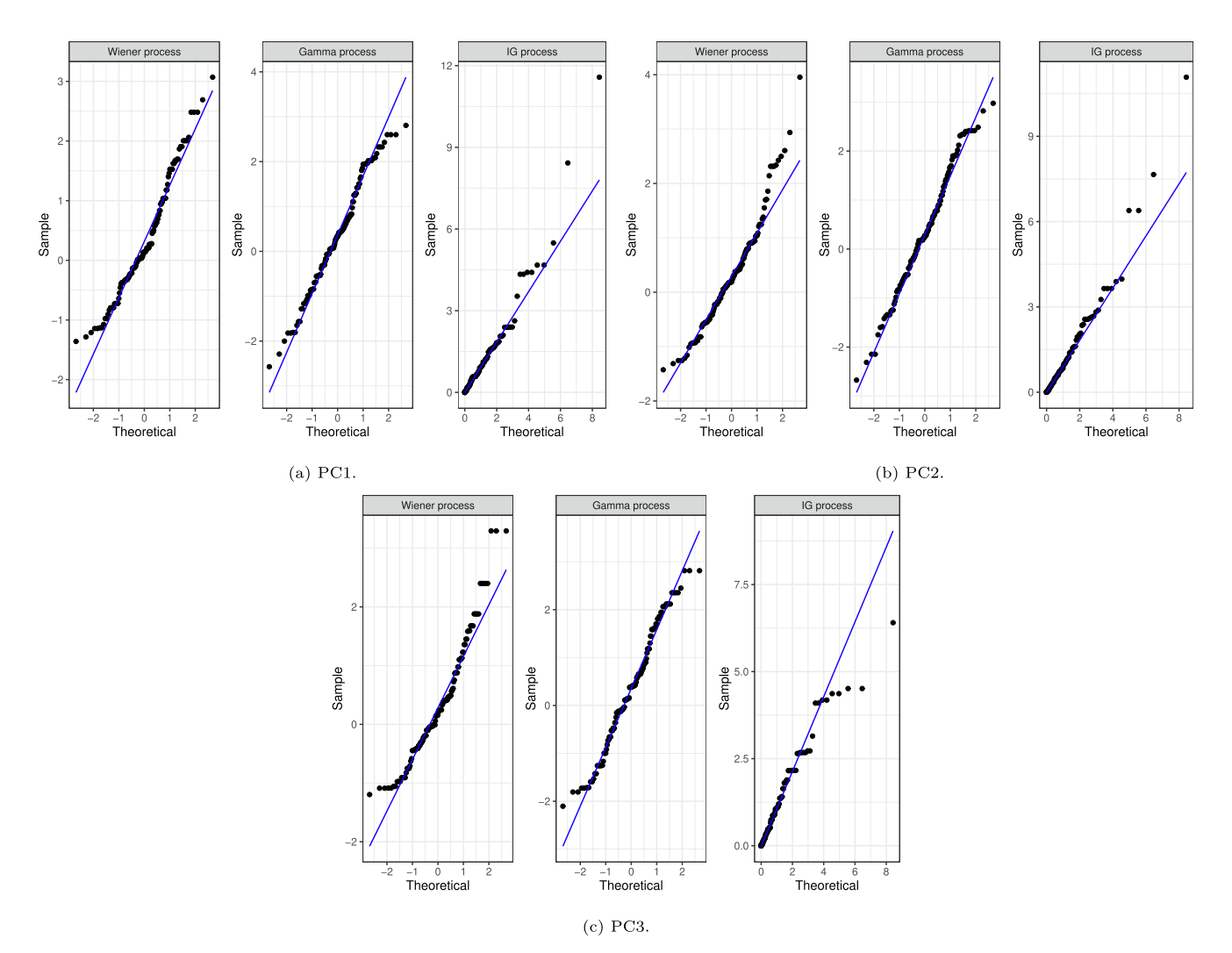


Fig. 9. QQ Plots for Various Marginal Degradation Models.

Table 2Results of Copula Fitting.

Model	Estimated Parameters	p-value of GOF test
Gaussian copula	$\hat{\rho}_{12} = 0.886, \hat{\rho}_{13} = 0.886, \hat{\rho}_{23} = 0.913$	0.007493
Student's t copula	$\widehat{\rho}_{12} = 0.886, \widehat{\rho}_{13} = 0.886, \widehat{\rho}_{23} = 0.913, \widehat{\nu} = 21.367$	0.008492
Exchangeable Frank copula	$\widehat{\delta} = 13.13$	0.01648
Exchangeable Clayton copula	$\widehat{\delta}=2.692$	0.0004995
Exchangeable Gumbel copula	$\widehat{\delta}=2.868$	0.009491
VC#1	$\widehat{\delta}_{12} = 2.790, \widehat{\delta}_{13} = 2.800, \widehat{\delta}_{23 1} = 1.510$	0.670
VC#2	$\widehat{\delta}_{12} = 2.820, \widehat{\delta}_{23} = 3.170, \widehat{\delta}_{13 2} = 1.280$	0.850
VC#3	$\hat{\delta}_{13} = 2.840, \hat{\delta}_{23} = 3.150, \hat{\delta}_{12 3} = 1.240$	0.535

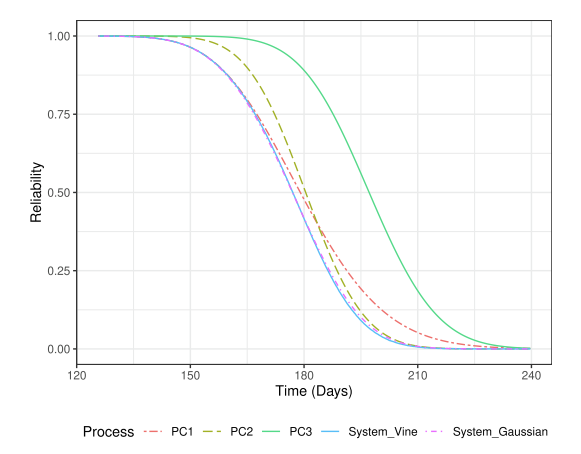


Fig. 11. Reliability Curves for Polymeric Materials.

photodegradation process due to exposure to certain levels of ultraviolet (UV) radiation, temperature, and relative humidity (RH). A bunch of ADTs were carried out on multiple test units, on which three different PCs (change of chemical structures at the wavelength of $1250~\rm cm^{-1}, 1510~\rm cm^{-1},$ and $2925~\rm cm^{-1})$ were measured repeatedly. For illustrative purposes, we arbitrarily select a subset of the data that were generated under the environmental setting – 100% UV intensity, 35° C, and 0% RH. The degradation paths are shown in Fig. 8, in which PC1, PC2, and PC3 represent the three PCs at the wavelength of $1250~\rm cm^{-1}, 1510~\rm cm^{-1},$ and $2925~\rm cm^{-1},$ respectively.

In the first step, we carry out parameters estimation for each PC. Since the MDPs are monotone, all the three marginal models described in Section 3.1 are considered as candidates. Note that since there may exist nonlinearity in these MDPs, it is necessary to apply the time scale transformation – $\Lambda(t;\gamma)=t^\gamma$. Table 1 provides the results of parameters estimation. It demonstrates that in terms of the AIC values the Wiener process provides the best fit for PC1 and PC2, while the gamma process provides the best fit for PC3. Fig. 9 indicates the corresponding QQ plots discussed in Section 5.2. It is obvious that most QQ plots indicate reasonable fit except the Wiener process for PC2 and PC3. Therefore, we choose the gamma process as the marginal models for PC2 and PC3 and the Wiener process as the marginal model for PC1.

Following the dependence analysis, we calculate pseudo-observations using the selected marginal models and generate a scatter plot to visualize dependence patterns. Fig. 10 shows the pairwise plots along with the estimated Kendall's τ , the estimated upper-tail

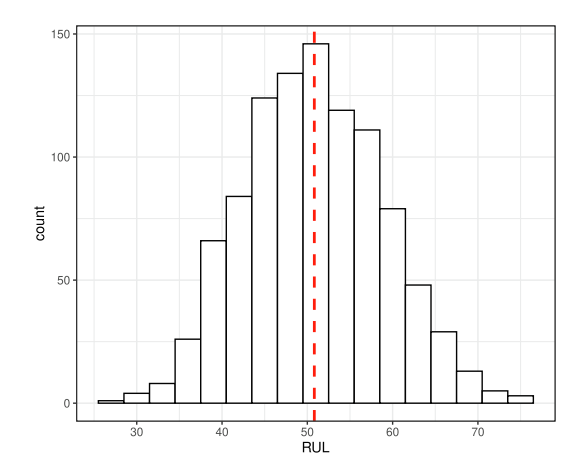


Fig. 12. Histogram of Predicted RULs for Unit 1.

dependence λ_U , and the estimated lower-tail dependence λ_L . It turns out all pairwise MDPs present an obvious strong upper-tail dependence, while a medium level of lower-tail dependence exists for PC2 v.s. PC3. By further conducting the test of independence mentioned in Section 5.2, rejection of the null hypothesis (i.e. MDPs are independent) is made due to extremely small p-value 0.0004995. These results confirm the dependency among MDPs, so we should proceed to the copula modeling step.

In the copula modeling step, we consider all the ECs, EACs, and VCs introduced before as candidate models. The step 2 of the IFM method is carried out to infer the unknown parameters. Particularly, for VCs, we include three different models according to three ways of joint pdf decomposition. Those are VC#1 ($c_{1,2}, c_{1,3}$, and $c_{2,3|1}$), VC#2 ($c_{1,2}, c_{2,3}$, and $c_{1,3|2}$), and VC#3 ($c_{1,3}, c_{2,3}$, and $c_{1,2|3}$). One can see that these three models vary in the choice of variable to be conditioned on for the conditional copula. In addition, observing that all pairwise MDPs indicate upper-tail dependence, we choose the Gumbel copula to model each bivariate copula in the VCs. Table 2 provides the results of copula fitting. Notice that none of ECs and EACs provides a reasonable fit due to the failure to pass the GOF test. Instead, all the VC models pass the GOF test. Furthermore, the AIC values are -519.166, -526.3189, and -525.0534 for VC#1, VC#2, and VC#3, respectively. Thus, we choose VC#2 as the multivariate degradation model due to the lowest AIC value. This result is intuitive since Fig. 10 has already shown the existing upper-tail dependence among all pairs of margins. Thus, fitting a symmetric or lower-tailed copula such as a Gaussian copula and an exchangeable Clayton copula is not appropriate. Also, due to the diverse magnitude of the Kendall's τ , fitting an exchangeable Gumbel copula that defines the same level of dependence for all pairwise margins is not proper too.

Next, following the discussion of reliability evaluation in Section 4.1, Fig. 11 provides reliability curves for the system. We assume the three PCs are in a series connection and their thresholds are $\mathcal{D}_1=-0.580,$ $\mathcal{D}_2=-0.660,$ and $\mathcal{D}_3=-0.380$ for PC1, PC2, and PC3, respectively. It also shows a deviated curve that results from modeling the data using the Gaussian copula.

Finally, following the RUL prediction discussed in Section 4.2, we generate 1,000 samples of predicted RULs for Unit 1 at intervals of 3 days. The histogram of these samples is given in Fig. 12. It turns out Unit 1 is predicted to survive for 50.82 additional days on average.

8. Discussion and conclusions

Degradation process, as accumulations of additive and irreversible damage, reflects a product's health status (Ye & Chen, 2014). When multiple degradation processes are affecting a system's performance, both uncertainty and dependence among performance measures usually

Table 3Basic Properties of Copula Theory.

	Bivaria	ate	Multivariate	
	cdf	pdf	cdf	pdf
Copula Scale:				
<u>u</u>				
Joint	$C(u_1,u_2)$	$c\left(u_1, u_2\right) = \frac{\partial^2 C(u_1, u_2)}{\partial u_1 \partial u_2}$ $f(u_i) = 1 \ \forall u_i \in [0, 1]$	$C(u_1,u_2,,u_d)$	$c(u_1, u_2,, u_d) = \frac{\partial^d C(u_1, u_2,, u_d)}{\partial u_1 \partial u_2 \cdots \partial u_d}$
Marginal	$U_i \sim \textit{Unif}(0,1)$	$f(u_i) = 1 \ \forall u_i \in [0,1]$	$U_i \sim \textit{Unif}(0,1)$	$f(u_i) = 1 \ \forall u_i \in [0,1]$
Conditional	$C(u_1 u_2) = \frac{\partial C(u_1,u_2)}{\partial u_2}$	$c(u_1,u_2)$	$\begin{split} C(u_1 u_2,,u_d) &= \frac{\partial C(u_1,u_2 u_3,,u_d)}{\partial u_2} \\ \overline{C}(u_1,u_2,,u_d) &= \sum_{J\subseteq \{1,,d\}} (-1)^{ J } C\Big((1-u_1)^{1(1\in J)},, \end{split}$	$c(u_1,u_2,,u_d)$
Survival	$\overline{C}(u_1,u_2) = u_1 + u_2 + \dots$	$c(1-u_1,1-u_2)$	$\overline{C}(u_1, u_2,, u_d) = \sum_{J \subseteq \{1,, d\}} (-1)^{ J } C((1 - u_1)^{1(1 \in J)},,$	$c(1-u_1,1-u_2,,1-u_d)$
	$C(1-u_1,1-u_2)-1$		$(1-u_d)^{1(d\in J)}$	
Original Conto				
<u>Scale:</u> <u>x</u> Joint	$F(x_1,x_2) = C(F_1(x_1),F_2(x_2))$	$f(x_1,x_2) = c(F_1(x_1),$ $F_2(x_2))f_1(x_1)f_2(x_2)$	$F(x_1,x_2,,x_d) = C(F_1(x_1),F_2(x_2),,F_d(x_d))$	$f(x_1, x_2,, x_d) = c(F_1(x_1), F_2(x_2),, F_d(x_d)) \prod_{i=1}^d f_i(x_i)$
Marginal	$F_i(x_i)$	$f_i(x_i)$	$F_i(oldsymbol{x}_i)$	$f_i(x_i)$
Conditional	$F_{1 2}(x_1 x_2) =$	$f_{1 2}(x_1 x_2) = c(F_1(x_1),$	$F(x \mathbf{x}^*) = \frac{\partial C_{\mathbf{x}.\mathbf{x}_j \mathbf{x}_{-j}^*} \left(F(\mathbf{x} \mathbf{x}_{-j}^*), F(\mathbf{x}_j \mathbf{x}_{-j}^*) \right)}{\partial F(\mathbf{x}_i \mathbf{x}^*)}$	$f(x x^*) = c_{x,x_j x_{-j}^*} (F(x x_{-j}^*), F(x_j x_{-j}^*)) f(x_j x_{-j}^*)$
	$\partial C(F_1(x_1),F_2(x_2))$	$F_2(x_2))f_1(x_1)$	$\partial F(x_j \hat{x_{-j}})$	$oldsymbol{x}_{-j}^*)$
Survival	$egin{aligned} rac{\partial F_2(x_2)}{ar F(x_1,x_2)} &= \ 1-F_1(x_1)-F_2(x_2) + \ C(F_1(x_1),F_2(x_2)) \end{aligned}$	$c(F_1(x_1),F_2(x_2))f_1(x_1) \\ f_2(x_2)$	$\overline{F}(x_1, x_2,, x_d) = \sum_{J \subseteq \{1,, d\}} (-1)^{ J } C(F_1(x_1)^{1(1 \in J)},, F_d(x_d)^{1(d \in J)})$	$c(F_1(x_1), F_2(x_2),, F_d(x_d)) \prod_{i=1}^d f_i(x_i)$

¹ For the cdf of survival copula, the sum extends over all 2^d subsets J of $\{1, ..., d\}$, |J| denotes the number of elements of J.

exist. From the application analyzed in the previous section and the examples mentioned in the introduction section, one can see that the interactions among multiple failure mechanisms imply the dependence existing in the multivariate degradation process. On the other hand, the degradation physics often suggests greater dependence in upper extreme direction. That is when a certain degradation process exhibits a worse state, it is more likely that other dependent processes would be affected to fall into a similarly risky status. For example, Chang, Das, Varde, and Pecht (2012) discussed how the LED lumen depreciation can be accelerated by severe discoloration, due to a reduction in the transparency of the encapsulants in LED package. Therefore, this close relation with system failure mechanisms provides a solid physical ground for the Gumbel copula to be chosen as a dependent degradation model. Similar logic applies to the Clayton copula as a dependent lifetime model (Hsu, Emura, & Fan, 2016; Bai, Shi, Liu, & Liu, 2018). In fact, the Gumbel copula is the only copula that is simultaneously Archimedean and max extreme-value (Genest & Rivest, 1989), which also rationalizes itself as a good model for describing the dependence structure between

exceptional events, i.e. degradation processes (Zhang, 2021).

Unlike the traditional Gaussian dependence-based models, including the multivariate general path model and the multivariate Wiener process model, the multivariate copula-based degradation models explored in this paper can tackle a wider range of applications. The flexibility in handling asymmetry, tail dependence and nonlinearity makes the copula-based modeling framework even more attractive in practice.

Beyond the scope of current study, there are several other issues worth of a further investigation.

- (1) Both unit-to-unit variations and explanatory variables may exist in the dependent degradation processes. Thus, incorporating random effects or covariates to both marginal and joint models is a future study direction.
- (2) Due to the complexity of degradation physics, both the dependence structure and magnitude may change over time. Thus, it is of much interest to further investigate a time-varying copula approach.

Table 4 Commonly-used ECs and EACs.

Copula	C(u)	Parameter(s)	Tail Dependence	Kendall's $ au$
Gaussian	$\Phi_{\Sigma} \big(\Phi^{-1}(u_1), \Phi^{-1}(u_2),, \Phi^{-1}(u_d) \big)$	$\Sigma > 0$	$\lambda_U = \lambda_L = 0$	$\tau = \frac{2}{\pi} \arcsin \rho$
Student's t	$T_{\Sigma_{\nu}}\big(T_{\nu}^{-1}(u_1),T_{\nu}^{-1}(u_2),\ldots,T_{\nu}^{-1}(u_d)\big)$	$oldsymbol{\Sigma} > 0, u > 2$	$\lambda_U = \lambda_L = 2T_{ u+1}\Biggl(rac{\sqrt{(u+1)(1- ho)}}{\sqrt{1+ ho}}\Biggr) \ \lambda_U = \lambda_L = 0$	$\tau = \frac{\pi}{\pi} \arcsin \rho$
Frank	$-\frac{1}{\delta} \ln \left\{ 1 + \frac{\left[\exp(-\delta u_1) - 1 \right] \left[\exp(-\delta u_2) - 1 \right] \cdots \left[\exp(-\delta u_d) - 1 \right]}{\left(\exp(-\delta) - 1 \right)^{d-1}} \right\}$	$\delta \in (-\infty,0) \bigcup (0,\infty)$	$\lambda_U = \lambda_L = 0$	$ au=1+4rac{D_1(\delta)-1}{\delta}$
Clayton	o $(\exp(-\delta)-1)^{\alpha-1}$ $(u_1^{-\delta}+u_2^{-\delta}+\cdots+u_d^{-\delta}-d+1)^{-1}$	$\delta \in [-1,\infty)/\{0\}$	$\lambda_U = 0, \lambda_L = 2^{-1/\delta}$	$ au = rac{\delta}{2+\delta}$
Gumbel	$\exp\Biggl\{-\left[\left(-\mathrm{ln}u_1\right)^{\delta}+\left(-\mathrm{ln}u_2\right)^{\delta}+\cdots+\left(-\mathrm{ln}u_d\right)^{\delta}\right]^{\dfrac{1}{\delta}}\Biggr\}$	$\delta \in [1,\infty)$	$\lambda_U=2{-}2^{1/\delta}, \lambda_L=0$	$ au=1$ $-1/\delta$

 $^{^{1}}$ $\Sigma > 0$ means Σ is a positive definite matrix and ρ is the correlation between two certain random variables.

 $^{^{2}\}overline{F}(x_{1},x_{2},...,x_{d})=P(X_{1}>x_{1},X_{2}>x_{2},...,X_{d}>x_{d}).$

 $^{^2}$ λ_U and λ_L are measures of upper-tail dependence and lower-tail dependence, respectively.

 $^{^{3}}D_{1}\left(\delta\right) = \frac{1}{\delta}\int_{0}^{\delta}\frac{t}{e^{t}-1}dt.$

Table 5
The Birst and Second Derivatives of Commonly, used Bive

The First and Second	The First and Second Derivatives of Commonly-used Bivariate Copulas.	
Copula	$h(u_1 u_2) = C(u_1 u_2) = \frac{\partial C(u_1,u_2)}{\partial u_2}$	$c(u_1,u_2)=\frac{\partial^2 C(u_1,u_2)}{\partial u_1 \partial u_2}$
Gaussian	$\Phi\left(\frac{\Phi^{-1}(u_1)-\rho\Phi^{-1}(u_2)}{\sqrt{1-\rho^2}}\right)$	$\frac{1}{\sqrt{1-\rho^2}} \exp \left\{ -\frac{\rho^2 \left(\Phi^{-1}(u_1)^2 + \Phi^{-1}(u_2)^2\right) - 2\rho\Phi^{-1}(u_1)\Phi^{-1}(u_2)}{2(1-\rho^2)} \right\}$
Student's t	$t_{\nu+1} \left(\frac{t_{\nu}^{-1}(u_1) - \rho t_{\nu}^{-1}(u_2)}{\left[\nu + \left[t_{\nu}^{-1}(u_2) \right]^2 \right] \left(1 - \rho^2 \right)} \right)$	$\frac{\Gamma\left(\frac{\nu+2}{2}\right)/\frac{\nu}{2}}{\nu r \cdot dt(t_{\nu}^{-1}(u_{1}),\nu) \cdot dt(t_{\nu}^{-1}(u_{1}),\nu) \cdot \sqrt{1-\rho^{2}}} \left\{1 + \frac{\left[t_{\nu}^{-1}(u_{1})\right]^{2} + \left[t_{\nu}^{-1}(u_{2})\right]^{2} - 2\rho t_{\nu}^{-1}(u_{1})t_{\nu}^{-1}(u_{2})}{\nu(1-\rho^{2})}\right\}$
Frank	$\frac{\varphi^{\delta}(e^{\delta n_1}+1)}{e^{\delta n_1\dots n_{\delta-\delta}(d(n+1),-\delta)}}$	$\frac{\delta(1-e^{-\delta})e^{-\delta(u_1+u_2)}}{(r_1-c_1)(r_1-c_2)(r_1-c_2)}$
Clayton	$u_2^{e^{-1}}(u_1^{-\delta} + u_2^{-\delta} - 1)^{-\frac{1}{\delta}}$	$(1-e^{-\nu}) - (1-e^{-\nu t_1})(1-e^{-\nu t_2}) = (1+\delta)(u_1u_2)^{-\delta-1}(u_1^{-\delta}+u_2^{-\delta}-1)^{-\delta} - 2$
Gumbel	$\exp\left\{-\left[(-\ln\!u_1)^\delta+(-\ln\!u_2)^\delta\right]^{\delta}\right\}\cdot \left[(-\ln\!u_1)^\delta+(-\ln\!u_2)^\delta\right]^{\frac{1}{\delta}}-1\left(-\ln\!u_2\right)^\delta/(u_2\ln\!u_2)$	$\exp\Biggl\{-\left[(-\ln u_1)^{\delta} + (-\ln u_2)^{\delta}\right]^{\delta}\Biggr\} \frac{1}{u_1u_2} \left[(-\ln u_1)^{\delta} + (-\ln u_2)^{\delta}\right]^{-2+} \frac{2}{\delta \cdot (\ln u_1 \ln u_2)^{\delta-1}} \left\{1 + (\delta-1)[(-\ln u_1)^{\delta} + (-\ln u_2)^{\delta}] \frac{1}{\delta}\right\}$

 ρ is the correlation between two certain random variables. $dt(\cdot, \nu)$ is the probability density of univariate t_{ν} distribution

- (3) It is noticed that for VCs, its flexibility originates from three elements graphical structure (i.e. trees), copula families for each edge, and copula parameters. In the numerical example, we enumerated all three possible structures and predetermined Gumbel copula for each edge. However, when dealing with a higher dimension and more complex degrading systems, it is not realistic to go through all possibilities. Thus, it is of interest to further develop a methodology to cover the general scenario.
- (4) In engineering practice, other than the degradation process, products may also be threatened by random shocks caused by sudden emergencies. Thus, to incorporate the effect of the shocks is necessary in the modeling framework. Some relevant works include (Cao, Liu, Fang, & Dong, 2020; Hao & Yang, 2018; Wang, Bai, & Zhang, 2020).
- (5) It is also noted that the simple series or parallel reliability-wise structure cannot cover many real examples, such as series-parallel and parallel-series systems. In such cases, the domain of a working system indicated in Fig. 1 would become much more complicated resulting in the difficulty in evaluating the multi-variate integral for characterizing system reliability. To deal with the problem, it is worthwhile to develop relevant methodologies or computing methods to overcome the challenge. Some relevant works include (Eryilmaz, 2011; Navarro, Ruiz, & Sandoval, 2007; Xu & Zhou, 2017).

CRediT authorship contribution statement

Guanqi Fang: Conceptualization, Methodology, Software, Validation, Writing - original draft. **Rong Pan:** Writing - review & editing, Supervision, Funding acquisition.

Declaration of Competing Interest

The authors declare that they have no known competing financial interests or personal relationships that could have appeared to influence the work reported in this paper.

Acknowledgment

The work by Fang was partially supported by the Characteristic & Preponderant Discipline of Key Construction Universities in Zhejiang Province (Zhejiang Gongshang University – Statistics). The work by Pan was partially supported by the National Science Foundation (NSF) grant 1726445.

Appendix A

Table 3 provides a summary of basic properties of copula theory. Table 4 provides a summary of commonly-used ECs and EACs. Table 5 provides a summary of the first and second derivatives of commonly-used bivariate copulas.

References

Aas, K., Czado, C., Frigessi, A., & Bakken, H. (2009). Pair-copula constructions of multiple dependence. *Insurance: Mathematics and Economics*, 44(2), 182–198.

Bae, S. J., & Kvam, P. H. (2004). A nonlinear random-coefficients model for degradation testing. *Technometrics*, 46(4), 460–469.

Bai, X., Shi, Y., Liu, Y., & Liu, B. (2018). Statistical analysis of dependent competing risks model in constant stress accelerated life testing with progressive censoring based on copula function. Statistical Theory and Related Fields, 2(1), 48–57.
 Bedford, T., & Cooke, R. M. (2001). Probability density decomposition for conditionally

Bedford, T., & Cooke, R. M. (2001). Probability density decomposition for conditionally dependent random variables modeled by vines. Annals of Mathematics and Artificial intelligence, 32(1-4), 245-268.

Bedford, T., & Cooke, R. M. (2002). Vines–A new graphical model for dependent random variables. The Annals of Statistics, 30(4), 1031–1068.

Brechmann, E., & Schepsmeier, U. (2013). CDVine: modeling dependence with C-and D-Vine copulas in R. *Journal of Statistical Software*, 52(3), 1–27.

- Cao, Y., Liu, S., Fang, Z., & Dong, W. (2020). Modeling ageing effects in the context of continuous degradation and random shock. *Computers & Industrial Engineering*, 145, 106539. ISSN 0360-8352.
- Castro, I. T., & Landesa, L. (2019). A dependent complex degrading system with non-periodic inspection times. Computers & Industrial Engineering, 133, 241–252. ISSN 0360-8352.
- Chang, M.-H., Das, D., Varde, P., & Pecht, M. (2012). Light emitting diodes reliability review. Microelectronics Reliability, 52(5), 762–782.
- Czado, C. (2019). Analyzing Dependent Data with Vine Copulas. Springer.
- Eryilmaz, S. (2011). Estimation in coherent reliability systems through copulas. Reliability Engineering & System Safety, 96(5), 564–568.
- Fang, G., Pan, R., & Hong, Y. (2020). Copula-based reliability analysis of degrading systems with dependent failures. *Reliability Engineering & System Safety*, 193, 106618.
 Fang. C. Birdon, S. E., & Pan, B. (2018). Predictive lifetime by degradation tests: A cope.
- Fang, G., Rigdon, S. E., & Pan, R. (2018). Predicting lifetime by degradation tests: A case study of ISO 10995. Quality and Reliability Engineering International, 34(6), 1228–1237.
- Genest, C., Quessy, J.-F., & Rémillard, B. (2007). Asymptotic local efficiency of Cramér–von Mises tests for multivariate independence. The Annals of Statistics, 35(1), 166–191.
- Genest, C., & Rémillard, B. (2004). Test of independence and randomness based on the empirical copula process. Test, 13(2), 335–369.
- Genest, C., & Rémillard, B. (2008). Validity of the parametric bootstrap for goodness-offit testing in semiparametric models. Annales de l'IHP Probabilités et statistiques, 44, 1096–1127.
- Genest, C., Rémillard, B., & Beaudoin, D. (2009). Goodness-of-fit tests for copulas: A review and a power study. Insurance: Mathematics and economics, 44(2), 199–213.
- Genest, C., & Rivest, L.-P. (1989). A characterization of Gumbel's family of extreme value distributions. Statistics & Probability Letters, 8(3), 207–211. ISSN 0167-7152.
- Hao, S., & Yang, J. (2018). Reliability analysis for dependent competing failure processes with changing degradation rate and hard failure threshold levels. *Computers & Industrial Engineering*, 118, 340–351. ISSN 0360-8352.
- He, D., Wang, Y., & Cao, M. (2018). Objective Bayesian analysis for the accelerated degradation model using Wiener process with measurement errors. Statistical Theory and Related Fields, 2(1), 27–36.
- He, L., Yue, R.-X., & He, D. (2018). Step-stress accelerated degradation test planning based on Wiener process with correlation. Statistical Theory and Related Fields, 2(1), 58-67
- Hsu, T.-M., Emura, T., & Fan, T.-H. (2016). Reliability inference for a copula-based series system life test under multiple type-I censoring. *IEEE Transactions on Reliability*, 65 (2), 1069–1080.
- Joe, H. (2005). Asymptotic efficiency of the two-stage estimation method for copulabased models. *Journal of Multivariate Analysis*, 94(2), 401–419.
- Killiches, M., Kraus, D., & Czado, C. (2017). Examination and visualisation of the simplifying assumption for vine copulas in three dimensions. Australian & New Zealand Journal of Statistics, 59(1), 95–117.
- Lawless, J., & Crowder, M. (2004). Covariates and random effects in a gamma process model with application to degradation and failure. *Lifetime Data Analysis*, 10(3), 213–227
- Lebrun, R., & Dutfoy, A. (2009). An innovating analysis of the Nataf transformation from the copula viewpoint. *Probabilistic Engineering Mechanics*, 24(3), 312–320.
- Li, H., Pan, D., & Chen, C. P. (2014). Reliability modeling and life estimation using an expectation maximization based Wiener degradation model for momentum wheels. *IEEE Transactions on Cybernetics*, 45(5), 969–977.
- Lu, L., Wang, B., Hong, Y., & Ye, Z. (2020). General Path Models for Degradation Data With Multiple Characteristics and Covariates. *Technometrics*, 1–16.
- Nagler, T., & Vatter, T. (2019). rvinecopulib: high performance algorithms for vine copula modeling, r package version 0.5.1.1.0.
- Navarro, J., Ruiz, J. M., & Sandoval, C. J. (2007). Properties of Coherent Systems with Dependent Components. Communications in Statistics - Theory and Methods, 36(1), 175–191
- Nelsen, R. B. (2007). An introduction to copulas. Springer Science & Business Media. Noh, Y., Choi, K., & Du, L. (2007). New transformation of dependent input variables using copula for RBDO. In 7th world congress on structural and multidisciplinary optimization, May, 21–25.
- Pan, Z., & Balakrishnan, N. (2011). Reliability modeling of degradation of products with multiple performance characteristics based on Gamma processes. *Reliability Engineering & System Safety*, 96(8), 949–957.
- Pan, R., & Fang, G. (2020). System Reliability Assessment with Multivariate Dependence Models. In L. Cui, I. Frenkel, & A. Lisnianski (Eds.), Stochastic Models in Reliability Engineering (pp. 19–39). CRC Press.

- Peng, C.-Y. (2015). Inverse Gaussian processes with random effects and explanatory variables for degradation data. *Technometrics*, 57(1), 100–111.
- Peng, W., Li, Y.-F., Yang, Y.-J., Zhu, S.-P., & Huang, H.-Z. (2016). Bivariate analysis of incomplete degradation observations based on inverse Gaussian processes and copulas. *IEEE Transactions on Reliability*, 65(2), 624–639.
- Peng, W., Ye, Z.-S., & Chen, N. (2018). Joint online RUL prediction for multivariate deteriorating systems. *IEEE Transactions on Industrial Informatics*, 15(5), 2870–2878.
- Segers, J. (2012). Asymptotics of empirical copula processes under non-restrictive smoothness assumptions. *Bernoulli*, 18(3), 764–782.
- Shen, L., Zhang, Y., Song, K., & Song, B. (2019). Failure analysis of a lock mechanism with multiple dependent components based on two-phase degradation model. *Engineering Failure Analysis*, 104, 1076–1093.
- Si, W., Yang, Q., Wu, X., & Chen, Y. (2018). Reliability analysis considering dynamic material local deformation. *Journal of Quality Technology*, 50(2), 183–197.
- Sun, F., Fu, F., Liao, H., & Xu, D. (2020). Analysis of multivariate dependent accelerated degradation data using a random-effect general Wiener process and D-vine Copula. *Reliability Engineering & System Safety*, 204, 107168.
- Wang, J., Bai, G., & Zhang, L. (2020). Modeling the interdependency between natural degradation process and random shocks. Computers & Industrial Engineering, 145, 106551, ISSN 0360-8352.
- Wang, X., Balakrishnan, N., & Guo, B. (2015). Residual life estimation based on nonlinear-multivariate Wiener processes. *Journal of Statistical Computation and Simulation*, 85(9), 1742–1764.
- Wang, X., Balakrishnan, N., Guo, B., & Jiang, P. (2015). Residual life estimation based on bivariate non-stationary gamma degradation process. *Journal of Statistical Computation and Simulation*, 85(2), 405–421.
- Wang, F., & Li, H. (2017). Towards reliability evaluation involving correlated multivariates under incomplete probability information: A reconstructed joint probability distribution for isoprobabilistic transformation. Structural Safety, 69, 1–10.
- Wang, F., & Li, H. (2018). System reliability under prescribed marginals and correlations: Are we correct about the effect of correlations? *Reliability Engineering & System Safety*, 173, 94–104.
- Wang, X., & Xu, D. (2010). An inverse Gaussian process model for degradation data. Technometrics. 52(2), 188–197.
- Whitmore, G., & Schenkelberg, F. (1997). Modelling accelerated degradation data using Wiener diffusion with a time scale transformation. *Lifetime Data Analysis*, *3*(1),
- Whitmore, G., & Seshadri, V. (1987). A heuristic derivation of the inverse Gaussian distribution. The American Statistician, 41(4), 280–281.
- Wu, S. (2014). Construction of asymmetric copulas and its application in twodimensional reliability modelling. *European Journal of Operational Research*, 238(2), 476–485.
- Xu, A., & Zhou, S. (2017). Bayesian analysis of series system with dependent causes of failure. Statistical Theory and Related Fields, 1(1), 128–140.
- Xu, D., Wei, Q., Elsayed, E. A., Chen, Y., & Kang, R. (2017). Multivariate degradation modeling of smart electricity meter with multiple performance characteristics via Vine copulas. *Quality and Reliability Engineering International*, 33(4), 803–821.
- Yan, J. (2006). Multivariate modeling with copulas and engineering applications. Springer Handbook of Engineering Statistics, 973–990.
- Yan, J. (2007). Enjoy the Joy of Copulas: with a package copula. *Journal of Statistical Software*, 21(4), 1–21.
- Yazdan Mehr, M., Bahrami, A., van Driel, W. D., Fan, X., Davis, J. L., & Zhang, G. (2020). Degradation of optical materials in solid-state lighting systems. *International Materials Reviews*, 65(2), 102–128.
- Ye, Z.-S., & Chen, N. (2014). The inverse Gaussian process as a degradation model. *Technometrics*, 56(3), 302–311.
- Ye, Z.-S., Wang, Y., Tsui, K.-L., & Pecht, M. (2013). Degradation data analysis using Wiener processes with measurement errors. *IEEE Transactions on Reliability*, 62(4), 772–780
- Ye, Z.-S., & Xie, M. (2015). Stochastic modelling and analysis of degradation for highly reliable products. *Applied Stochastic Models in Business and Industry*, 31(1), 16–32.
- Zhai, Q., & Ye, Z.-S. (2017). Robust degradation analysis with non-Gaussian measurement errors. *IEEE Transactions on Instrumentation and Measurement*, 66(11), 2803–2812.
- Zhang, Z. (2021). On studying extreme values and systematic risks with nonlinear time series models and tail dependence measures. Statistical Theory and Related Fields, 5 (1), 1–25.